

The transcriptional activator GCN4 contains multiple activation domains that are critically dependent on hydrophobic amino acids.

C M Drysdale, E Dueñas, B M Jackson, U Reusser, G H Braus and A G Hinnebusch
Mol. Cell. Biol. 1995, 15(3):1220.

Updated information and services can be found at:
<http://mcb.asm.org/content/15/3/1220>

CONTENT ALERTS

These include:

Receive: RSS Feeds, eTOCs, free email alerts (when new articles cite this article), [more»](#)

Information about commercial reprint orders: <http://journals.asm.org/site/misc/reprints.xhtml>
To subscribe to to another ASM Journal go to: <http://journals.asm.org/site/subscriptions/>

The Transcriptional Activator GCN4 Contains Multiple Activation Domains That Are Critically Dependent on Hydrophobic Amino Acids

CONNIE MARIE DRYSDALE,¹ ENCARNACION DUEÑAS,¹ BELINDA M. JACKSON,¹ UELI REUSSER,²
GERHARD H. BRAUS,^{2,3} AND ALAN G. HINNEBUSCH^{1*}

Section on Molecular Genetics of Lower Eukaryotes, Laboratory of Molecular Genetics, National Institute of Child Health and Human Development, Bethesda, Maryland 20892¹; Mikrobiologisches Institut, ETH-Zentrum, CH-8092 Zürich, Switzerland²; and Institut für Mikrobiologie, Biochemie & Genetik, Friedrich Alexander Universität, D-91058 Erlangen-Nürnberg, Germany³

Received 20 September 1994/Returned for modification 3 November 1994/Accepted 1 December 1994

GCN4 is a transcriptional activator in the bZIP family that regulates amino acid biosynthetic genes in the yeast *Saccharomyces cerevisiae*. Previous work suggested that the principal activation domain of GCN4 is a highly acidic segment of approximately 40 amino acids located in the center of the protein. We conducted a mutational analysis of GCN4 with a single-copy allele expressed under the control of the native promoter and translational control elements. Our results indicate that GCN4 contains two activation domains of similar potency that can function independently to promote high-level transcription of the target genes *HIS3* and *HIS4*. One of these domains is coincident with the acidic activation domain defined previously; the other extends over the N-terminal one-third of the protein. Both domains are partially dependent on the coactivator protein ADA2. Each domain appears to be composed of two or more small subdomains that have additive effects on transcription and that can cooperate in different combinations to promote high-level expression of *HIS3* and *HIS4*. At least three of these subdomains are critically dependent on bulky hydrophobic amino acids for their function. Five of the important hydrophobic residues, Phe-97, Phe-98, Met-107, Tyr-110, and Leu-113, fall within a region of proposed sequence homology between GCN4 and the herpesvirus acidic activator VP16. The remaining three residues, Trp-120, Leu-123, and Phe-124, are highly conserved between GCN4 and its *Neurospora* counterpart, *cpc-1*. Because of the functional redundancy in the activation domain, mutations at positions 97 and 98 must be combined with mutations at positions 120 to 124 to observe a substantial reduction in activation by full-length GCN4, and substitution of all eight hydrophobic residues was required to inactivate full-length GCN4. These hydrophobic residues may mediate important interactions between GCN4 and one or more of its target proteins in the transcription initiation complex.

Stimulating gene transcription in eukaryotic organisms typically involves binding of a specific activator protein at one or more locations upstream of the TATA sequence, the site where TATA box-binding protein (TBP) nucleates the assembly of basic transcription factors and RNA polymerase II (reviewed in reference 5). Several molecular mechanisms have been considered to explain how activators stimulate transcription. One possibility is an alteration of chromatin structure in the vicinity of the TATA element in a way that facilitates assembly of the transcription initiation complex. Other models involve recruitment of a general transcription factor to the promoter or antagonizing a repressor of one of the basic transcription factors. It has also been suggested that activators can stimulate a rate-limiting step in the initiation process or prevent the formation of a nonproductive initiation complex (12, 52). For most of these mechanisms, it is frequently envisioned that activators interact directly with one of the basic transcription factors, such as TBP or TFIIB, and there is evidence to support this view (8, 20, 33, 34, 36, 46, 47). There are also indications, however, that activators interact with the basic factors through mediators or coactivators, some of which appear to be stably associated with TBP (10, 11, 16) or with the core subunits of RNA polymerase II (23, 26). In the case of the yeast transcriptional activator GCN4, two proteins known as

ADA2 (2) and GCN5 (9) have been implicated as coactivators, but their modes of action in mediating activation by GCN4 are unknown.

GCN4 is a transcriptional activator of genes encoding amino acid biosynthetic enzymes in more than 10 different pathways in *Saccharomyces cerevisiae*. Expression of *GCN4* is regulated at the translational level, with the result that high levels of the protein are synthesized in response to amino acid deprivation. The GCN4 protein thus produced increases the transcription of amino acid biosynthetic genes under its control and thereby ameliorates the limitation for amino acids (reviewed in reference 14). GCN4 is a member of the bZIP family of transcriptional activators (28) that binds to DNA as a homodimer (19). The DNA-binding and dimerization domain (bZIP) of GCN4 is ca. 56 amino acids in length and is located at the extreme C terminus of the protein (7, 18, 40). The 225 amino acids N terminal to the bZIP region of GCN4 are largely dispensable for sequence-specific DNA binding and contain the residues required for transcriptional activation of GCN4 target genes (18).

Extensive deletion analysis of GCN4 led to the conclusion that the principal activation function resided in a segment located roughly in the center of the protein, between residues 107 and 144, that is rich in acidic amino acids and carries a net negative charge. It was proposed that this region contains an array of negatively charged alpha-helical segments that make additive contributions to the efficiency of transcriptional acti-

* Corresponding author. Phone: (301) 496-4480. Fax: (301) 496-0243.

vation (17, 18). However, recent results with circular dichroism spectroscopy suggested that the central activation domain of GCN4 is not alpha-helical in solution and can adopt a β -sheet structure under certain conditions (54). The deletion analysis of Hope et al. (17) provided some evidence for a weaker activation function in GCN4 between residues 12 and 92, in that low-level activation of a *lexA*-dependent promoter occurred when the N-terminal third of GCN4 and a small segment of the central activation domain were fused in the same molecule to the *lexA* DNA-binding domain. In addition, Pellman et al. (42) found that deletion of the N-terminal 95 amino acids of GCN4, leaving the central activation domain intact, reduced both the efficiency of transcriptional activation and its dependence on a TATA element at *HIS4*. These latter results suggested that the N-terminal region of GCN4 might make an important contribution to transcriptional activation, even though it did not appear to be sufficient to promote wild-type levels of transcription from GCN4-dependent promoters.

In previous mutational studies on GCN4, the relative levels of mutant proteins were not determined because GCN4 expressed in *S. cerevisiae* was undetectable immunologically (17). This made it difficult to compare different segments of the protein for their efficiency of transcriptional activation. In addition, the *GCN4* alleles were expressed constitutively from heterologous promoters, and it was unknown how their protein levels compared with that of wild-type GCN4. In our study, we examined mutations made in a single-copy *GCN4* gene containing the native promoter and translational control elements, after inducing the expression of each allele by amino acid starvation. The levels of wild-type and mutant GCN4 proteins thus produced were quantitated by immunodetection. In view of different requirements observed for the potential coactivator GCN5 in GCN4-mediated transcriptional activation of *HIS3* versus *HIS4* (9), we analyzed the effects of our *GCN4* mutations on the authentic promoters of these two *HIS* genes rather than assaying synthetic promoters containing multiple binding sites inserted upstream of a TATA element.

Using these tools, we set out to determine whether the central acidic activation domain (CAAD) defined by Hope et al. (17) was actually necessary for efficient transcription of authentic GCN4 target genes under physiological conditions of induction. This inquiry was motivated partly by the fact that one of the activation domains identified in the yeast transcriptional activator GAL4 was found to be dispensable for activation of *GAL* genes in vivo (29, 35). A related goal was to make a careful comparison of the relative efficiencies of transcriptional activation conferred by the CAAD and sequences N-terminal to the CAAD and to map the boundaries of the putative N-terminal activation domain (NTAD). On the basis of evidence that different segments of the GCN4 activation domain may interact differently with factors bound at the TATA element (42), we wished to compare the NTAD and CAAD for dependence on the coactivator ADA2. Finally, because activation domains in VP16 (6, 45), the Rta activator of Epstein-Barr virus (13), p53 (32), the Sp1 activator (10), c-Fos (36), E1A (31), and yeast GAL4 (30) all contain hydrophobic residues that are important for the activation functions of these proteins, we wanted to determine whether this structural feature extended to GCN4.

The results presented below indicate that the NTAD confers high-level transcriptional activation of *HIS3* or *HIS4* in the absence of the CAAD. Similarly, the CAAD can promote high-level transcription of these genes when the NTAD is missing. Both the CAAD and the NTAD are dependent on the ADA2 protein for efficient transcriptional activation at *HIS3* and at *HIS4*. Both the NTAD and CAAD appear to contain

two or more autonomously functioning subdomains which have cumulative effects on transcription, and at least three of these subdomains contain amino acids with bulky hydrophobic side chains that are critical for activation and are interspersed among acidic residues. Elimination of all three clusters of hydrophobic residues was required to destroy the activation function of full-length GCN4. These results indicate that the activation domain of GCN4 is more complex than was previously thought and that it shares significant structural similarities with activation domains found in several other well-studied transcriptional activators.

MATERIALS AND METHODS

Construction of plasmids. All mutant constructs were derived from plasmid pCD35, containing the wild-type *GCN4* allele on a 2.8-kb *SalI-EcoRI* genomic fragment inserted into YCp50 (39). pCD35 was derived from plasmid p298 (57) by first removing the *Bam*HI fragment containing the *lacZ* coding sequences and then replacing the *SalI-Bst*EII fragment containing the *GCN4* mRNA leader sequences with the corresponding *SalI-Bst*EII fragment from p164 (38). The in-frame linker insertion mutations shown in Fig. 2A were constructed with the Stratagene Mutator Kit, following the instructions of the vendor. The 1.2-kb *SalI-KpnI* and 1.6-kb *KpnI-EcoRI* *GCN4* fragments were individually subcloned into M13mp19. Single-stranded DNA was prepared and annealed with phosphorylated oligonucleotides complementary to the appropriate *GCN4* coding sequences, plus the additional nucleotides AGATCT, to create a *Bgl*II site. Double-stranded DNA from M13 clones bearing the desired insertions was subcloned into pCD35, either as *SalI-KpnI* or *KpnI-EcoRI* fragments. All subcloned fragments and the immediately flanking regions were sequenced in their entirety to verify the mutations.

The deletion mutations in constructs pCD105, pCD108, pCD109, pCD110, pCD112, pCD115, pCD116, pCD121, pCD122, pCD123, pCD124, pCD125, pCD162, pCD213, pCD214, pCD216, pCD316, p1588, and p1589 were made by combining fragments containing *Bgl*II sites obtained from the appropriate linker insertion mutations. Construct pCD196 was generated by cloning the *SalI-XbaI* fragment of pCD122 between the *SalI-XbaI* sites in pCD116. Construct pCD316 contained the following nucleotide changes to generate the desired alanine substitutions at Phe-97 and Phe-98, plus a silent mutation at Ser-100 to facilitate subcloning: an F-to-A change at position 97 (F97A; TTC to GCC), F98A (TTT to GCT), and S100S (TCA to TCT).

Constructs pCD345, pCD346, pCD349, and pCD357 were generated by a recombinant PCR technique (21). These constructs contained the following nucleotide changes to generate the desired amino acid substitutions. pCD345 contains M107A (ATG to GCC), Y110A (TAT to GCT), and L113A (CTA to GCG); pCD346 contains the same mutations present in pCD345 plus W120A (TGG to GCG), L123A (TTG to GCG), and F124A (TTT to GCT); pCD349 contains W120A (TGG to GCG), L123A (TTG to GCG), and F124A (TTT to GCT); and pCD357 contains W120A (TGG to GCG). In pCD345, pCD346, pCD349, and pCD357 the following silent mutations were also introduced to facilitate subcloning: I128I (ATT to ATA), P129P (CCA to CCG), V130V (GTT to GTA), V135V (GTT to GTA), and S136S (TCA to AGC).

To generate constructs pCD313, pCD314, pCD317, pCD318, pCD319, pCD320, pCD321, pCD322, pCD323, and pCD324, 75-mer oligonucleotides with *Bgl*II ends were synthesized and inserted into the *Bgl*II site of pCD125, pCD108, or pCD315. (pCD315 has the same deletion as pCD108 plus the identical point mutations present in pCD297.) This scheme generated an additional *Bgl*II linker (Arg-Ser codon) between positions 117 and 118. The sequences of the inserted oligonucleotides, plus flanking nucleotides, were confirmed by DNA sequencing. The following list gives the sequence changes in this set of constructs: pCD314, wild-type sequences; pCD317, M107A (ATG to GCG); pCD318, Y110A (TAT to GCT); pCD319, L113A (CTA to GCA); pCD313, M107A (ATG to GCG), Y110A (TAT to GCT), and L113A (CTA to GCA); pCD320, E109A (GAG to GCG), E111A (GAA to GCA), E114A (GAA to GCA), and D115A (GAC to GCC).

In producing constructs pCD270, pCD271, and pCD272, DNA fragments were synthesized by PCR with oligonucleotides designed to create the appropriate deletions and to generate restriction sites at the ends of the fragments for subcloning between the *XbaI* and *Bgl*II sites of pCD122. The same was done to generate constructs pCD269, pCD257, pCD261, pCD282, and pCD283, by inserting the appropriate PCR-generated DNA fragments into the *Bgl*II site of pCD214. Similarly, constructs pCD294, pCD295, pCD296, pCD297, and pCD298 were produced by inserting PCR-generated fragments between the *Bam*HI (codon 54 in *GCN4*) and *Bgl*II sites of pCD162. The following amino acid changes, plus silent mutations, were made in constructs pCD294 to -298: pCD294, F97A (TTC to GCC) and S100S (TCA to TCT); pCD295, F98A (TTT to GCT) and S100S (TCA to TCT); pCD296, S99A (TCG to GCG) and S100S (TCA to TCT); pCD297, F97A (TTC to GCC), F98A (TTT to GCT), and S100S (TCA to TCT); and pCD298, V93A (GTA to GCA) and S100S (TCA to TCT). For constructs pCD273 and pCD274, PCR-generated fragments containing

*Bam*HI and *Bgl*II ends were cloned between the *Bam*HI and *Bgl*II sites of pCD162. Constructs pCD350, pCD353, pCD355, and pCD356 were constructed by combining fragments containing *Bgl*II ends from pCD297 or pCD162 with fragments containing *Bgl*II ends from pCD349, pCD345, or pCD346.

In producing constructs pCD327 and pCD328, DNA fragments were synthesized by PCR with oligonucleotides complementary to wild-type *GCN4* sequences and containing additional nucleotides to create *Bgl*II ends. These small fragments were cloned into pCD214. All regions of DNA generated by PCR, plus immediately flanking nucleotides, were confirmed by DNA sequencing.

All versions of *GCN4* alleles lacking the four upstream open reading frames (uORFs; pCD118, pCD171, pCD288, pCD291, and p1617) were constructed by substituting the wild-type 0.645-kb *Sall*-*Bst*EII fragment of the appropriate uORF-containing construct with the *Sall*-*Bst*EII fragment from p238 (38) containing point mutations that eliminate the ATG codons of all four uORFs.

The production of plasmids for in vitro transcription of *GCN4* coding sequences from the bacteriophage SP6 promoter began with the construction of plasmid p250. A 1.8-kb *Sca*I fragment containing the *GCN4* coding region and point mutations in all four uORFs was isolated from plasmid p238 (38) and inserted at the *Hinc*I site of plasmid pSP64 (Promega), yielding p250. The appropriate segments containing coding regions from the *GCN4* constructs of interest were then isolated and inserted in place of the corresponding wild-type segments of p250.

The *LEU2* integrating plasmid pCD215 containing the *HIS4-lacZ* fusion was constructed with plasmid pAB177 (provided by K. Arndt) that contains 750 nucleotides of sequence 5' to the *HIS4* coding region and the first 11 codons of *HIS4* fused in frame to the *Escherichia coli lacZ* gene. First, plasmid pCD151 was produced by deleting the sequences between the *Not*I and *Nae*I sites of pRS314 (50) and subsequently inserting a 3-kb *Bam*HI fragment containing the *lacZ* gene obtained from plasmid pMC1871 (48) into the *Bam*HI site of the polylinker. Second, the 1.6-kb *Cla*I fragment containing the *HIS4* promoter and 830 nucleotides of *lacZ* sequence was isolated from pAB177 and inserted into the *Cla*I site of pCD151 to produce pCD173. The *Sal*I (filled in with Klenow)-*Bss*HIII fragment of pCD173, containing *HIS4-lacZ* fusion sequences, was then inserted into the *Sma*I-*Bss*HIII site of pDK215 (24), a *LEU2* integrating vector, to generate pCD215. The *TRP1* integrating plasmid, containing the *HIS4-lacZ* fusion, was generated by subcloning the *Bam*HI-*Kpn*I fragment of pCD173, containing the *HIS4-lacZ* fusion described above, into the *Bam*HI-*Kpn*I site of pRS304, a *TRP1* integrating vector (50), generating p1622. The *TRP1* integrating plasmid p1623, containing the *HIS3-lacZ* fusion, was generated by first subcloning the *Sma*I-*Bss*HIII fragment from pDK215 (24) into the *Sma*I-*Bss*HIII site of pCD151, described above, generating pCD164. The *Bam*HI fragment of pCD164, containing the entire *HIS3-lacZ* fusion, was then inserted into the *Bam*HI site of pRS304 (50). The construct pCD250 contains the *GAL4-VP16* fusion protein on a high-copy-number *URA3* vector. This was generated by subcloning the *Bam*HI fragment of padhGV16 (2) into the *Bam*HI site of pRS426 (50).

Construction of yeast strains. Strain H2036 (*MATa ura3-52 gcn4-103 leu2-3 leu2-112 trp1-63 ino1*) was constructed by crossing yeast strain H384 bearing *gcn4-103* (38) with a laboratory strain containing the appropriate auxotrophic markers. The *gcn4-103* allele in H2036 is a deletion of 0.645 kb between the *Kpn*I site in the *GCN4* coding region and the *Mlu*I site located 3' of the gene and was constructed previously (38). Integrating *LEU2* plasmids containing *HIS4-lacZ* or *HIS3-lacZ* fusions, pCD215 and pDK215 (24), respectively, were linearized at the *Kpn*I site in *LEU2* and used individually to transform *S. cerevisiae* H2036 to *Leu*⁺, generating strains H2384 (*MATa ura3-52 gcn4-103 leu2-3 leu2-112 trp1-63 ino1* [*HIS3-lacZ LEU2*]) and H2359 (*MATa ura3-52 gcn4-103 leu2-3 leu2-112 trp1-63 ino1* [*HIS4-lacZ LEU2*]). Integration of the plasmids at *LEU2* was confirmed by DNA blot hybridization analysis. Strain H2032 (*MATa ura3-52 his1-29 leu2-3 leu2-112 trp1-63 gcn4::LEU2*) was constructed by crossing strain H1663 (*MATa ura3-52 leu2-3 leu2-112 his1-29 gcn4::LEU2 ino1-13*) with a laboratory strain containing the appropriate auxotrophic markers. The *gcn4::LEU2* allele in H1663 contains a 2.8-kb *LEU2* fragment inserted in *GCN4* between positions +90 and +1095 relative to the 5' end of *GCN4* mRNA (36a). To generate the *ada2Δ* deletion strain H2483 (*MATa ada2Δ ura3-52 his1-29 leu2-3 leu2-112 trp1-63 gcn4::LEU2*), strain H2032 was transformed to *Ura*⁺ with a *Bam*HI-*Xho*I fragment containing the *ada2Δ* allele in which the C-terminal 395 codons of *ADA2* were replaced by the *URA3* gene flanked by *hisG* direct repeats, isolated from plasmid pada2Δ (2). *Ura*⁺ transformants were grown in the presence of 5-fluoroorotic acid (3) to select for loss of the *URA3* gene, yielding the unmarked *ada2* allele.

Strains H2452 (*MATa ura3-52 leu2-3 leu2-112 trp1-63 his1-29 gcn4::LEU2* [*HIS4-lacZ TRP1*]) and H2453 (*MATa ura3-52 leu2-3 leu2-112 trp1-63 his1-29 gcn4::LEU2* [*HIS3-lacZ TRP1*]) were generated by transforming strain H2032 with plasmids p1622 and p1623, respectively, selecting for tryptophan prototrophy. Strains H2505 (*MATa ada2Δ ura3-52 leu2-3 leu2-112 trp1-63 his1-29 gcn4::LEU2* [*HIS4-lacZ TRP1*]) and H2506 (*MATa ada2Δ ura3-52 leu2-3 leu2-112 trp1-63 his1-29 gcn4::LEU2* [*HIS3-lacZ TRP1*]) were generated from strains H2452 and H2453, respectively, by deleting *ADA2* in the same way described for H2483. We verified that the slow-growth phenotype on rich medium associated with deletion of *ADA2* in strains H2483, H2505, and H2506 was complemented by transformation with the low-copy-number plasmid pNS3.8 (2) bearing wild-type *ADA2*. Additionally, these strains showed suppression of the slow-growth phenotype conferred by high-level expression of the *GAL4-VP16* fusion protein

from pCD250, relative to that seen in the parental *ADA2* strains. The isogenic strains BP1 (*MATa ura3-52 ade1-100 his4-519 leu2-2 leu2-112 gal4::HIS4*) and BP1/ada2-1 (*MATa ada2-1 ura3-52 ade1-100 his4-519 leu2-2 leu2-112 gal4::HIS4*) were described previously (2). As expected from the work of Berger et al. (2), padhGV16 was lethal in the *ADA2* strain but not in its *ada2-1* derivative. Strain H1486 (*MATa ura3-52 his1-29 leu2-3 leu2-112* [*HIS4-lacZ ura3-52*]) has been previously described (56).

All *GCN4* constructs derived from pCD35 were introduced by transformation into strains H2032, H2036, H2359, H2384, H2452, H2453, H2483, H2505, and H2506 by selecting for uracil prototrophy.

Immunoblot analysis of GCN4 proteins expressed in *S. cerevisiae*. *GCN4* protein levels in transformants of *S. cerevisiae* H2359 were measured in whole-cell extracts as follows. Transformants were grown to saturation at 30°C in SC medium (49) lacking uracil (SC-Ura) and inoculated at a 1/100 dilution into 50 ml of SC lacking uracil and histidine (SC-Ura-His). Cultures were grown to an optical density at 546 nm of 1.0, and 3-aminotriazole (3-AT) was added to 40 mM. Cultures were harvested 12 to 14 h later by centrifugation at 4°C in 50-ml centrifuge tubes half-filled with crushed ice at 3,000 rpm for 7 min. Cells were washed with 2.5 ml of ice-cold breaking buffer (B buffer; 100 mM Tris-Cl [pH 7.5], 200 mM NaCl, 20% glycerol, 5 mM EDTA) containing 14 mM β-mercaptoethanol, 0.5 mM *Nα-p*-tosyl-L-lysine chloromethyl ketone, 0.5 mM *Nα-p*-tosyl-L-phenylalanine chloromethyl ketone, 0.5 mM *p*-aminobenzamide-HCl, 0.5 mM *o*-phenanthroline, and 0.5 mM phenylmethylsulfonyl fluoride (B buffer+) added immediately prior to use. All subsequent steps were carried out at 4°C. Cells were pelleted at 3,000 rpm for 7 min and resuspended in B buffer+ and transferred to 1.5-ml microcentrifuge tubes pre-filled with 250 μl of acid-washed glass beads. Samples were vortexed for six periods of 15 s (each) with 1 min of cooling on ice between each period. Occasionally, an additional 200 μl of B buffer+ was added, and the sample was vortexed for an additional 15 s. Samples were centrifuged for 15 min at 14,000 rpm in a microcentrifuge, and the supernatant was centrifuged as before for 15 min. The supernatants were divided into aliquots, frozen immediately in liquid N₂, and stored at -70°C. Protein concentration was determined by the Bradford (4) method with reagent purchased from Bio-Rad. Samples were boiled for 3 min in 2× or 6× Laemmli sample buffer (27), depending on the protein concentration, and cooled on ice prior to fractionation by sodium dodecyl sulfate (SDS)-8 to 16% polyacrylamide gel electrophoresis (PAGE). Proteins were electroblotted to nitrocellulose filters at 4°C in 1× Laemmli running buffer (per liter: 29 g of Tris base, 144 g of glycine, and 10 g of SDS)-20% methanol for 2 h in a Novex XCell Mini-Cell transfer apparatus at 6 W, 35 V, and 125 mA. The filters were washed briefly in 1× phosphate-buffered saline (PBS), blocked overnight in PBS-milk (1× PBS, 2% Carnation nonfat dry milk, 0.02% Na₂S₂O₈) at 4°C, and incubated for 1 h at the ambient temperature in PBS-milk containing *GCN4*-specific antiserum at a 1:100 dilution. The filters were washed four times for 5 min (each) in PBS-milk and incubated for 1 h in PBS-milk containing 1:2,000 alkaline phosphatase-conjugated goat anti-rabbit immunoglobulin G heavy plus light chains obtained from Bio-Rad. Subsequently, the filters were washed three times for 5 min (each) in PBS and 1 time for 5 min in 08-15 buffer (100 mM K-glycine [pH 9.5], 10 mM MgCl₂) and then stained in 15 ml of 08-15 buffer containing 5-bromo-4-chloro-indoxylphosphate at 0.1 mg/ml and nitrotetrazolium blue at 0.14 mg/ml, without agitation and with protection from light. The blots were washed briefly with water to stop the reaction and photographed.

The *GCN4* antibodies were raised in a rabbit against a synthetic peptide containing the 60 C-terminal amino acids of *GCN4*. The peptide was linked to keyhole limpet hemocyanin with glutaraldehyde and injected subcutaneously after being mixed with an equal volume of incomplete Freund's adjuvant. After 5 weeks, additional injections (six times, once per week) served as boosters.

Immunoblot analysis of GCN4 proteins synthesized in vitro. Mutant and wild-type *GCN4* proteins were synthesized by in vitro transcription of the appropriate *GCN4* constructs, using SP6 RNA polymerase (43). Equivalent volumes of the transcription reaction mixture were translated in rabbit reticulocyte lysates by established procedures (43), using 40 μCi of [³⁵S]methionine (Amersham; 1,200 Ci/mmol) for each 50-μl in vitro translation reaction mixture. No attempt was made to quantitate mRNAs from individual transcription reaction mixtures. Samples were boiled for 3 min in 2× Laemmli sample buffer, cooled on ice, and fractionated by SDS-8 to 16% PAGE. Proteins were electroblotted to nitrocellulose filters, incubated with *GCN4*-specific antiserum and alkaline phosphatase-conjugated goat anti-rabbit immunoglobulin G heavy plus light chains, and stained as described above. The same blots were subjected to autoradiography for comparing the amounts of ³⁵S-labeled total protein with the amounts of the corresponding proteins detected by immunoblot analysis.

Assays of β-galactosidase expressed from *HIS3-lacZ* and *HIS4-lacZ* fusions. Transformants of strains H2505, H2506, H2359, H2384, H2452, and H2453 bearing the appropriate *GCN4* constructs were grown for 2 days to saturation in SD medium (49) supplemented with 0.2 mM inositol, 2.0 mM leucine, 0.5 mM isoleucine, 0.5 mM valine, 0.4 mM tryptophan, and 0.25 mM arginine and diluted 1:50 into the same medium. For starvation conditions, 3-AT was added to 10 mM after 2 h of growth, and cultures were harvested 6 h later. Starvation of the *ADA2* and *ada2Δ* strains could not be established by the addition of 3-AT, since these strains harbor a leaky *HIS1* mutation; therefore, sulfometuron methyl (55) was added to 5 μg/ml for the same period of time to starve for isoleucine and valine. Whole-cell extracts were prepared, and β-galactosidase specific activities were

determined as previously described (37). The values obtained for each construct are the averages obtained from replicate determinations on at least three independent transformants, with standard errors of 10% or less. The β -galactosidase activities measured for a large number of transformants of strain H2359 or H2384 bearing vector YCp50 alone were averaged and equated with the GCN4-independent component of expression from each of these fusions. These two values were subtracted from the activities measured in transformants of the appropriate strain (H2359 or H2384) bearing the *GCN4* construct of interest to yield the GCN4-dependent component of fusion enzyme expression for that construct. The GCN4-dependent expression conferred by each construct was expressed as the percentage of GCN4-dependent expression measured for the wild-type allele on pCD35.

RESULTS

The central acidic activation domain of GCN4 is not required for efficient transcriptional activation in the presence of the N-terminal activation domain. We wished to determine whether the CAAD, mapped previously to residues 107 to 144 (17), is necessary for efficient transcriptional activation of *HIS3* and *HIS4* when GCN4 is expressed at physiological levels. To answer this question, we constructed a set of internal deletions in a *GCN4* allele that contains the native promoter and four uORFs that mediate translational induction of GCN4 protein under amino acid starvation conditions. Each plasmid-borne mutant allele was introduced into strains deleted for chromosomal *GCN4* and containing an integrated *HIS3-lacZ* or *HIS4-lacZ* fusion. To determine the effects of the deletions on GCN4-mediated activation, we measured the ability of each allele to confer growth on medium containing 3-AT, an inhibitor of the *HIS3* gene product. Transcriptional activation of *HIS3* (and possibly other genes in the histidine pathway) is required for resistance to 3-AT at the concentrations we employed (15). For most mutant alleles, we also assayed the β -galactosidase activity expressed from the *HIS4-lacZ* and *HIS3-lacZ* fusions after growing cells in the presence of 3-AT to induce translation of *GCN4* mRNA. For most constructs, the levels of GCN4 proteins produced in cells treated with 3-AT were measured by immunoblot analysis of whole-cell extracts, using GCN4-specific antibodies. Differences in the levels of mutant versus wild-type proteins were quantitated by determining the relative amounts of mutant and wild-type extracts that contain equivalent amounts of GCN4 protein. Our antibodies were raised against the C-terminal 60 amino acids of GCN4 containing the DNA-binding domain, and immunoblot analysis of selected mutant proteins synthesized in rabbit reticulocyte lysates showed that even large deletions in the activation domain did not affect the efficiency of immunodetection with this antiserum (Fig. 1).

We analyzed two-codon insertions (AGA-TCT) and relatively small deletions constructed from these insertions and found that only those mutations affecting the dimerization/DNA-binding (bZIP) domain led to a substantial reduction in transcriptional activation by GCN4 (pCD46 and pCD47 in Fig. 2A and pCD115 in Fig. 2E; see also Fig. 3). These three alleles had a 3-AT sensitivity phenotype indistinguishable from that of the vector alone. Deletions affecting other regions of the protein had only minor effects on 3-AT resistance and led to no reduction in *HIS4-lacZ* expression. In fact, *HIS4-lacZ* expression was elevated above the wild-type level for all the deletions that removed segments of the CAAD (Fig. 2B). Interestingly, the deletions in pCD124 (Fig. 2C), pCD112, and pCD116 (Fig. 2D) reduced *HIS3-lacZ* expression but not that of the *HIS4-lacZ* fusion. This more severe effect on *HIS3-lacZ* versus *HIS4-lacZ* expression was seen for many additional alleles described below and may indicate that the *HIS3* promoter has a more stringent requirement for GCN4 activation functions than does *HIS4*.

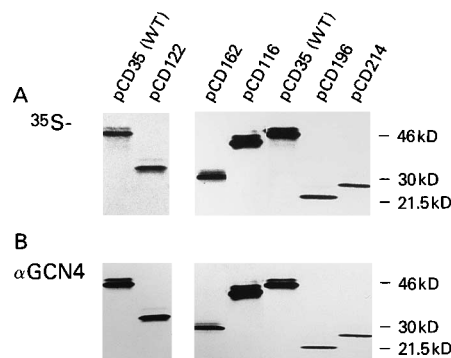


FIG. 1. Immunoblot analysis of wild-type (WT) and mutant GCN4 proteins synthesized in vitro. [35 S]methionine-labeled GCN4 proteins were synthesized in rabbit reticulocyte lysates from transcripts produced in vitro for the indicated constructs. (A) The labeled proteins were separated by SDS-8 to 16% PAGE, transferred to nitrocellulose filters, and visualized by autoradiography. (B) The identical filters used for panel A were probed with GCN4-specific antiserum (α GCN4), and the immune complexes were visualized with alkaline phosphatase-conjugated goat anti-rabbit serum. An identical analysis was also performed on mutant proteins derived from pCD108, pCD109, pCD110, pCD122, pCD123, pCD125, pCD213, and pCD215 (data not shown). All of the latter proteins were recognized by the antiserum to very similar extents, with the exception of the pCD108- and pCD123-encoded proteins, which gave ca. two-fold-higher levels of immune complexes than were expected from the amounts of the radiolabeled proteins detected on the filter.

In light of previous results (17, 18), it was surprising that the CAAD could be substantially truncated or completely removed (Fig. 2B, pCD123 and pCD162) without causing any decrease in transcriptional activation of *HIS4* and a reduction in *HIS3-lacZ* expression of only ca. 10%. These findings indicated that GCN4 contains one or more additional activation domains that can promote high-level transcription when the CAAD is completely missing, as for pCD162. Immunoblot analysis indicated, however, that the pCD162 protein accumulates to levels about fourfold higher than that of wild-type GCN4 (Fig. 2B and 4A), raising the possibility that the postulated activation determinants in this construct do not function as efficiently as those located in the CAAD. Because the pCD162 protein accumulates to higher levels than wild-type GCN4, it might occupy more of the available binding sites at GCN4 target genes and thereby achieve wild-type activation. This interpretation is at odds with the following two observations. First, the pCD123 activator lacks most of the CAAD, as it was defined previously (17, 18) and below, and yet it shows wild-type transcriptional activation, even though it is present at levels lower than the wild-type level (Fig. 2B and 4B). The second observation came from analyzing constructs in which three different large segments of GCN4 were fused to the bZIP domain in an effort to map segments of the protein that are sufficient for transcriptional activation (Fig. 2F and 3). As expected, the construct containing the bZIP region and only the N-terminal 17 amino acids of GCN4 (pCD216) had no activation function. Essentially the same result was obtained for pCD214, which additionally contains the 49 residues immediately N terminal to the bZIP domain. In contrast, significant activation of *HIS4-lacZ* was seen for pCD196, in which the segment between 101 and 169 containing the CAAD was fused directly to the bZIP domain. Similar results were obtained for pCD213, containing the first 100 residues of the protein fused to bZIP. Immunoblot analysis indicated that all four of these proteins were present at levels comparable to one another but lower than that of wild-type GCN4 (Fig. 2F and 4C). Together, these results suggested that the middle segment

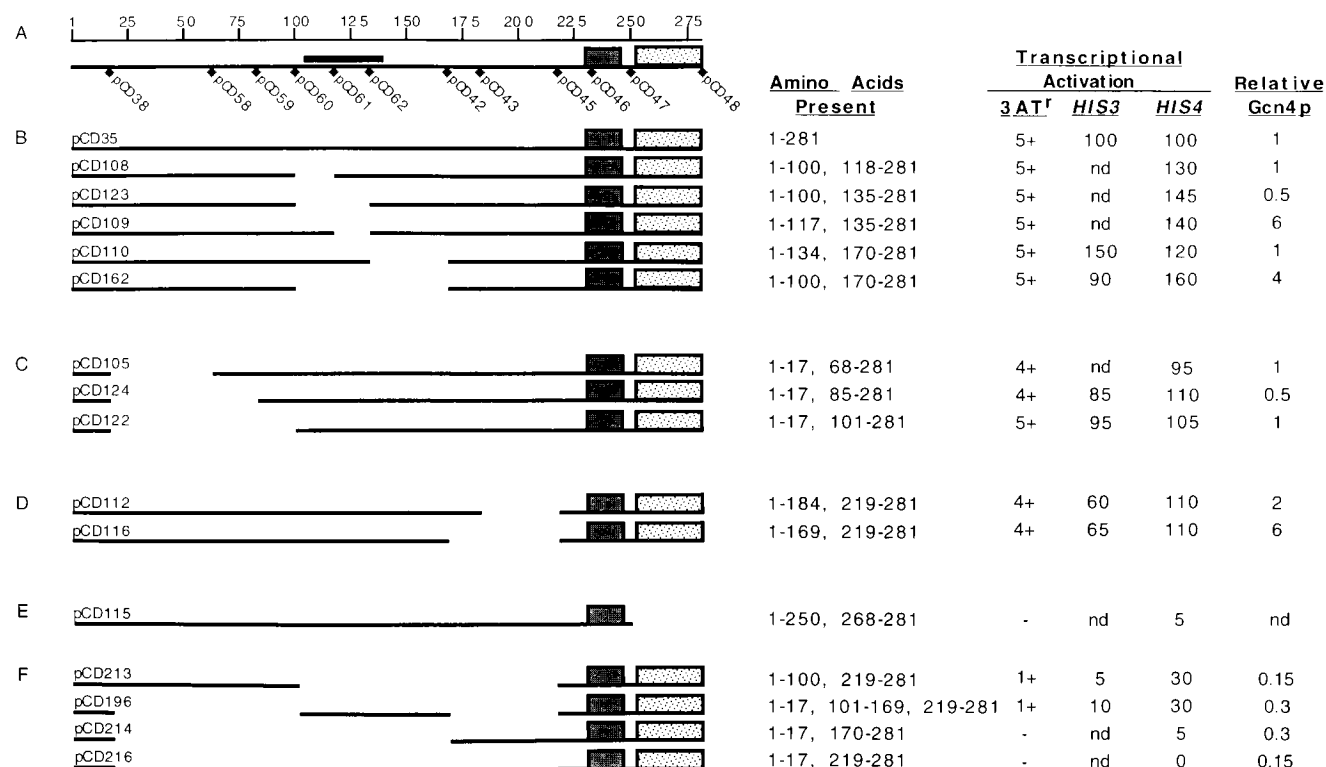


FIG. 2. Effects of two-codon insertions and deletions in *GCN4* on transcriptional activation and the levels of GCN4 protein under histidine starvation conditions. (A) Two-codon insertions in GCN4. The linear amino acid sequence of GCN4 is shown as a solid line with the DNA-binding and leucine zipper segments of the bZIP domain shown as shaded and stippled rectangles, respectively, at the C terminus. The location of the CAAD as defined by Hope et al. (17) is indicated by a solid bar above the sequence. Amino acid positions relative to the N terminus are shown on the ruler line at the top. The locations of in-frame Arg-Ser codon insertions (AGA-TCT) that introduce *Bgl*III sites into the coding sequence are shown as solid diamonds below the sequence of GCN4. The following list gives the amino acid positions interrupted by the two-codon insertions for the indicated constructs: pCD38, 17-18; pCD58, 67-68; pCD59, 84-85; pCD60, 100-101; pCD61, 117-118; pCD62, 134-135; pCD42, 169-170; pCD43, 184-185; pCD45, 218-219; pCD46, 234-235; pCD47, 250-251; and pCD48, the Arg-Ser codons are at the C terminus. All of the insertion mutations conferred wild-type resistance to 3-AT, except for pCD46 and pCD47, which had a 3-AT sensitivity phenotype indistinguishable from that of vector alone. (B, C, D, E, and F) In-frame deletions constructed by joining pairs of *Bgl*III sites from the various insertion alleles shown in panel A. Transformants of strain H2359 bearing the indicated constructs were tested for the ability to derepress *HIS* genes subject to *GCN4* control by growth on 3-AT plates, as described in the legend to Fig. 3. Growth was scored relative to those of the wild-type construct pCD35 (5+) and the vector YCp50 alone (-). Transcriptional activation of *HIS3* and *HIS4* was determined by assaying *HIS3-lacZ* and *HIS4-lacZ* fusions in transformants of strains H2384 and H2359, respectively, under conditions of histidine starvation induced with 3-AT. Expression of *HIS3-lacZ* and *HIS4-lacZ* under histidine starvation conditions was reduced to 20 to 25% of wild-type levels when no GCN4 protein was present. This GCN4-independent expression is attributable to different basal transcriptional control elements at these two genes (14). Therefore, the GCN4-independent component of *HIS4-lacZ* and *HIS3-lacZ* expression was subtracted from the observed results, and only the GCN4-dependent component of transcriptional activation for each allele is presented. Expression of each fusion is given as the percentage of that conferred by the wild-type construct pCD35 in the same strain. The levels of GCN4 proteins (Relative Gcn4p) under histidine starvation conditions were measured by immunoblot analysis of whole-cell extracts of H2359 transformants bearing the indicated constructs, as described in the legend to Fig. 4. nd, not determined.

of GCN4 containing the CAAD and the N-terminal segment of the protein each contain activation functions that are roughly equivalent in strength.

The pCD213 and pCD196 constructs shown in Fig. 2F contain the same activation segments present in pCD162 and pCD122, shown in Fig. 2B and C, respectively, but do not activate transcription as effectively as these latter two constructs do. We attribute this difference partly to the fact that the pCD213 and pCD196 proteins accumulate to lower levels than do the pCD162 and pCD123 products, because we found that the pCD213 and pCD196 proteins confer levels of activation of *HIS3* and *HIS4* higher than wild-type levels when they are overexpressed (data not shown). In addition, the pCD213 and pCD196 proteins also lack amino acids 170 to 218 immediately upstream of the bZIP domain, and removing this segment from an otherwise wild-type *GCN4* allele was found to reduce transcriptional activation at *HIS3* (pCD116 [Fig. 2D]). Presumably, this region of the GCN4 protein increases the efficiency of transcriptional activation by the CAAD and NTAD.

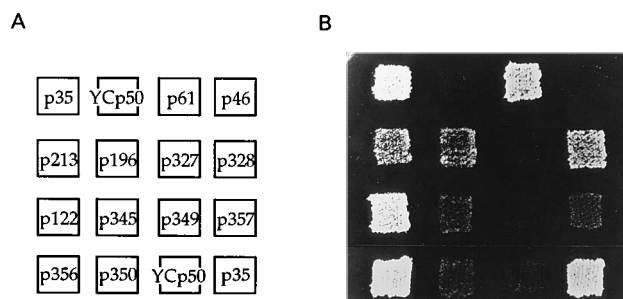


FIG. 3. Effects of *GCN4* mutations on the derepression of histidine biosynthetic genes. (A) Transformants of strain H2359 containing the wild-type *GCN4* allele (pCD35), the vector YCp50 alone, or the indicated *GCN4* mutant alleles were tested for the ability to grow in the presence of 3-AT. (B) Patches of transformants were grown to confluence on synthetic medium supplemented with all 20 amino acids and lacking uracil (SC-Ura plates), and replica plated to SC-Ura plates or to SC-Ura plates lacking histidine and containing 10 mM 3-AT and incubated for 2 days at 30°C. All transformants grew at the same rate as the wild type on SC-Ura plates (data not shown).

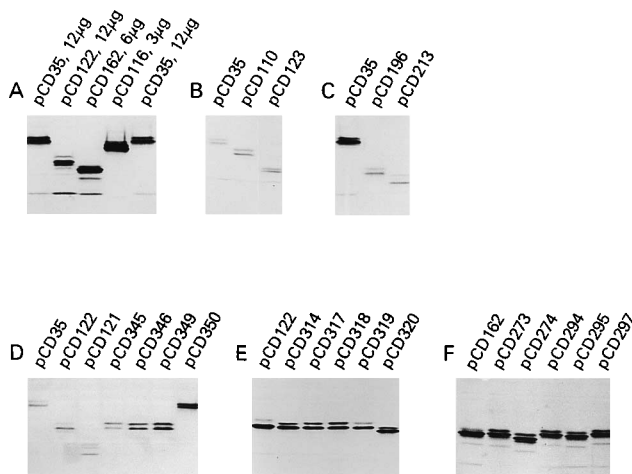


FIG. 4. Immunoblot analysis of mutant and wild-type GCN4 proteins expressed in *S. cerevisiae*. (A) Aliquots containing protein from whole-cell extracts prepared from transformants of strain H2359 containing the wild-type allele on pCD35, the indicated mutant *GCN4* constructs, or vector alone were separated by SDS-8 to 16% PAGE, electroblotted to nitrocellulose filters, and probed with GCN4-specific antiserum. Immune complexes were visualized with alkaline phosphatase-conjugated goat anti-rabbit serum. (B) Twice the amount of total protein from pCD123 extracts was immunoblotted compared with that in the pCD35 and pCD110 extracts. (C, D, E, and F) Equivalent amounts of total protein from the extracts was immunoblotted.

Analysis of hydrophobic and acidic residues in the CAAD.

We sought to determine whether the activation function detected in the 101 to 169 interval (the CAAD) is coincident with the acidic activation domain that was previously mapped to residues 107 to 144 by Hope et al. (17). To verify the C-terminal boundary of the CAAD, we constructed nested deletions in construct pCD122, which is completely dependent on the CAAD for transcriptional activation (Fig. 5A). A comparison of constructs with similar protein levels (pCD270 with pCD271 and pCD122 with pCD272 [Fig. 5A]) suggested that the C-terminal boundary of the CAAD maps between positions 139 and 154, close to the boundary identified previously (17). We also obtained results consistent with the reported location of the N-terminal boundary of the CAAD. The deletion in pCD125 reduces expression of *HIS4-lacZ* and *HIS3-lacZ* to 45 and 10% of wild-type levels, respectively, without reducing the level of GCN4 protein relative to that of the parental construct pCD122 (Fig. 5A). These results indicate that an important activation determinant is located between residues 101 and 118. Deletion of roughly three-fourths of the CAAD in construct pCD121 reduced *HIS4-lacZ* expression to 20% of the wild-type level and completely abolished GCN4-dependent *HIS3-lacZ* expression. The residual activation of *HIS4-lacZ* seen with pCD121 was essentially eliminated by deleting the entire CAAD (Fig. 5A, pCD214). Although these latter two deletions reduced the levels of GCN4 protein (Fig. 4D and 5A), the comparison of construct pCD214 with pCD213 and pCD196 in Fig. 2F indicates that the pCD214 protein is produced at levels sufficient to detect activation, whereas essentially none was detected. It is noteworthy that the deletions of the CAAD in constructs pCD125, pCD121, and pCD214 which impaired activation function (Fig. 5A) had little effect on transcription when made in the complete GCN4 protein (pCD108, pCD123, and pCD162 [Fig. 2B]). This suggests either that the N-terminal activation domain compensates for these mutations or that residues 118 to 170 are non-functional in the context of the full-length protein. Results supporting the former explanation will be presented below.

Mutational analysis of the VP16 acidic activation domain had indicated that hydrophobic residues were critical for transcriptional activation and led to the suggestion that an important sequence motif composed of interspersed acidic and bulky hydrophobic residues was loosely conserved between VP16 and other acidic activators, including a segment in GCN4 (6, 45). The C-terminal two-thirds of this proposed motif is located in GCN4 near the N terminus of the CAAD and contains the hydrophobic residues Met-107, Tyr-110, and Leu-113 (Fig. 5D). The deletion in pCD125 (Fig. 5A) removes 17 amino acids encompassing these three hydrophobic amino acids and the surrounding acidic residues and led to significantly reduced transcriptional activation by the CAAD. Another short stretch of amino acids located just C terminal to the proposed VP16 motif in GCN4 (Trp-120 Thr-121 Ser-122 Leu-123 Phe-124 [Fig. 5D]) represents the longest stretch of consecutive residues (four of five) conserved between the activation domains of GCN4 and its *Neurospora crassa* counterpart, *cpc-1* (41). Removal of this latter block of amino acids by the deletion in pCD121 further reduced transcriptional activation relative to that of the pCD125 construct (Fig. 5A). For these reasons, we asked whether the conserved hydrophobic residues in these two contiguous segments were important for activation by the CAAD.

To answer this question, we constructed multiple alanine substitutions of the hydrophobic residues in construct pCD122, which lacks the NTAD and depends entirely on the CAAD for transcriptional activation. Construct pCD345, lacking Met-107, Tyr-110, and Leu-113, is substantially impaired for activation (Fig. 5B and 3) and shows the same low-level function observed upon deletion of these residues in construct pCD125 (Fig. 5A). Construct pCD349, lacking residues Trp-120, Leu-123, and Phe-124, which are conserved between GCN4 and *cpc-1*, is even more impaired than pCD345, showing no activation of *HIS3* and only 15% of the wild-type activation of *HIS4* (Fig. 5B and 3). Substitution of all six hydrophobic residues in pCD346 completely inactivated this protein. None of these point mutations decreased the levels of GCN4 protein (Fig. 4D), showing that the hydrophobic amino acids are required for GCN4 function and not for expression or stability of the protein. These results suggest that the CAAD contains two activation subdomains between positions 107 and 124 that contain hydrophobic residues as critical constituents. Both subdomains are required for *HIS3* expression, whereas the segment containing Met-107, Tyr-110, and Leu-113 can be removed without reducing *HIS4* transcription to low levels.

To produce individual substitutions at Met-107, Tyr-110, and Leu-113, we used a derivative of pCD122 containing an additional *Bgl*III insertion in the CAAD that led to a decrease in *HIS3* transcription (compare pCD314 in Fig. 5C with pCD122 in Fig. 5B). Thus, the size or structure of the region separating the two hydrophobic clusters in the CAAD may contribute to the efficiency of activation. Substitution of Met-107, Tyr-110, and Leu-113 with alanines in pCD314 had nearly the same phenotype seen for the triple-alanine substitution in pCD122 (compare pCD313 and pCD345 in Fig. 5B and C). Each of the single-alanine substitutions of the three hydrophobic residues in constructs pCD317 to pCD319 reduced activation less than was seen for the triple substitution in pCD313 (Fig. 5C), with replacement of Tyr-110 showing the greatest effect. We also found that alanine substitutions at all four acidic residues located between 107 and 115 (pCD320) reduced activation somewhat less than occurred with the triple substitution of the hydrophobic residues within this interval in pCD313 (Fig. 5C). None of these point mutations led to decreases in the level of GCN4 protein (Fig. 4E and 5C). Thus,

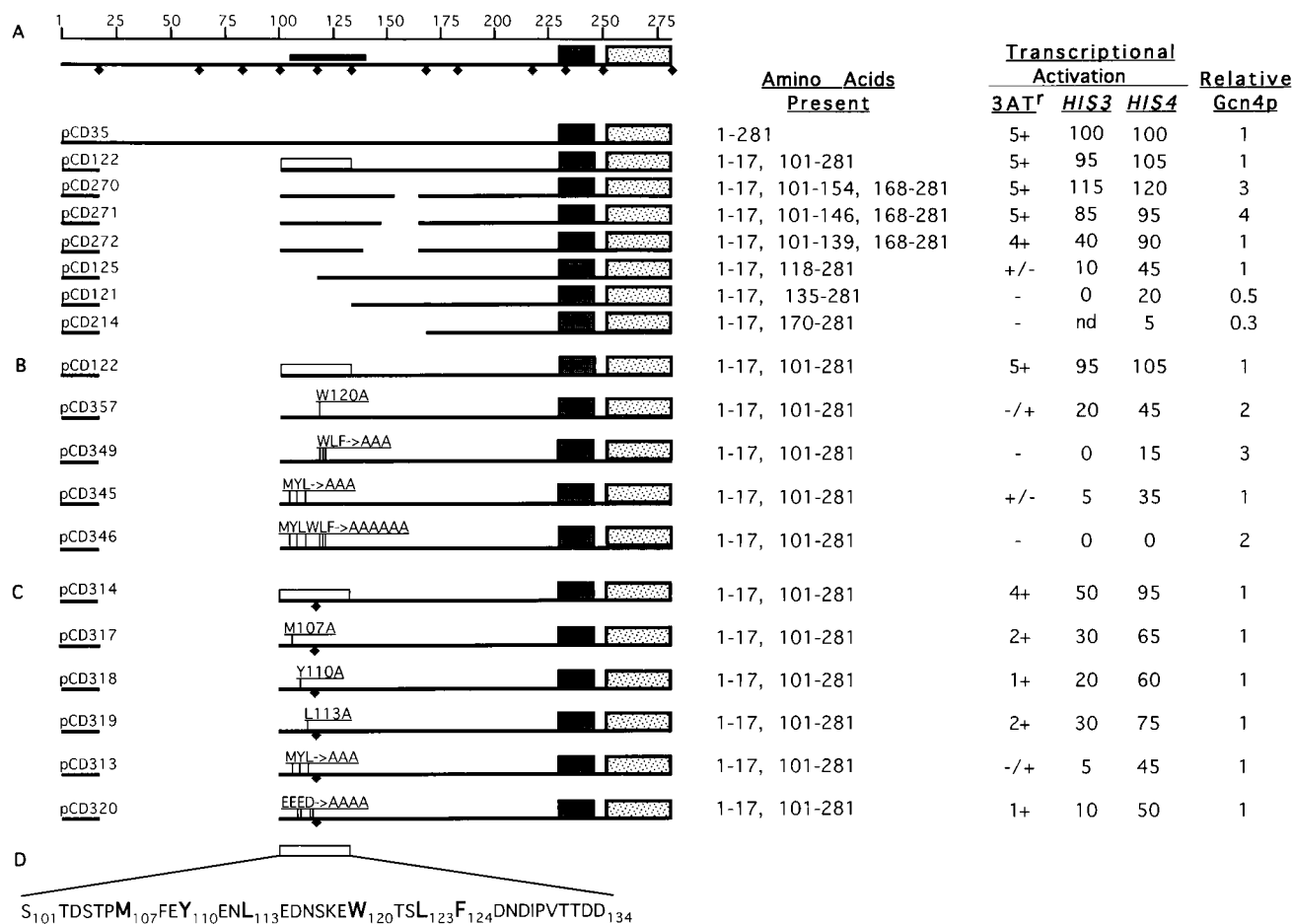


FIG. 5. Mutational analysis of the CAAD. The schematics and presentation of results are all as described in the legend to Fig. 2, except for the following additions. (A) The open rectangle shown on construct pCD122 (and on pCD122 and pCD314 in lower panels) gives the location of the amino acid sequence shown in panel D. (B) Construct pCD357 contains a single-alanine substitution for Trp-120, as indicated with the single-letter amino acid code and the location of the residue in GCN4. Construct pCD349 contains alanine substitutions of Trp-120, Leu-123, and Phe-124, and construct pCD345 contains alanine substitutions of Met-107, Tyr-110, and Leu-113. pCD346 contains all six alanine substitutions present in pCD345 and pCD349. (C) The constructs all contain a *Bgl*III site (solid diamond shown below the sequence) inserted between residues 117 and 118. The single-alanine substitutions introduced at Met-107, Tyr-110, and Leu-113 in constructs pCD317 to pCD319 are indicated as described above. All three substitutions are present together in construct pCD313. In construct pCD320, Glu-109, Glu-111, Glu-114, and Asp-115 were all changed to alanine. (D) Amino acid sequence of GCN4 between residues 101 and 134, containing the C-terminal portion of the sequence motif proposed by Cress and Triezenberg (6) containing Met-107, Tyr-110, and Leu-113, plus the adjacent residues conserved between GCN4 and *Neurospora* *cpc-1* (41), including Trp-120, Leu-123, and Phe-124. nd, not determined. Growth on 3-AT plates was scored relative to the wild-type construct pCD35 (5+) and the vector alone (-) with intermediate values of 4+, 3+, 2+, 1+, +/-, and -/+, in descending order.

each of the three hydrophobic residues at positions 107, 110, and 113 and the intervening acidic amino acids in the 107 to 115 interval in the N terminus of the CAAD make important contributions to its activation function. Interestingly, a single-alanine substitution of Trp-120 in the *cpc-1*-related motif impaired activation by the CAAD to a greater extent than was seen for any of the three single-alanine substitutions at Met-107, Tyr-110, or Leu-113 (compare pCD357 in Fig. 5B with the data in Fig. 5C). Although Trp-120 is a critical constituent of its subdomain, a comparison of constructs pCD357 and pCD349 (Fig. 5B and 3) indicates that Leu-123 or Phe-124 also contributes to activation by this segment of the CAAD.

Analysis of hydrophobic residues in the NTAD. We attempted to identify the boundaries of the NTAD by making deletions in a construct that lacks the CAAD and depends entirely on the NTAD for transcriptional activation. The parental construct for these deletions (pCD269 [Fig. 6A]) was a derivative of pCD162 (Fig. 6B) containing a *Bgl*III site inserted at amino acid position 17. This insertion alone led to a mea-

surable decrease in *HIS3* and *HIS4* expression relative to that of the parental construct pCD162, without lowering the level of protein, thus suggesting that the NTAD contains an activation determinant located close to the N terminus of GCN4. Additional support for this conclusion came from the fact that deletion of residues 18 to 24 from the site of the *Bgl*III insertion reduced activation relative to that of pCD269 without decreasing the level of GCN4 protein (pCD257 [Fig. 6A]). The next deletion (construct pCD261) did not reduce activation relative to pCD257 but lowered protein accumulation to essentially wild-type levels. Deletion of 15 more residues from pCD261, producing pCD282, led to another drop in activation without an additional decrease in the GCN4 protein level (Fig. 6A), indicating that a second activation determinant in the NTAD spans positions 33 to 47. Because significant activation remained intact in construct pCD282, it appears that additional activation determinants are present in the NTAD between residues 48 and 100.

We investigated the C-terminal boundary of the NTAD by

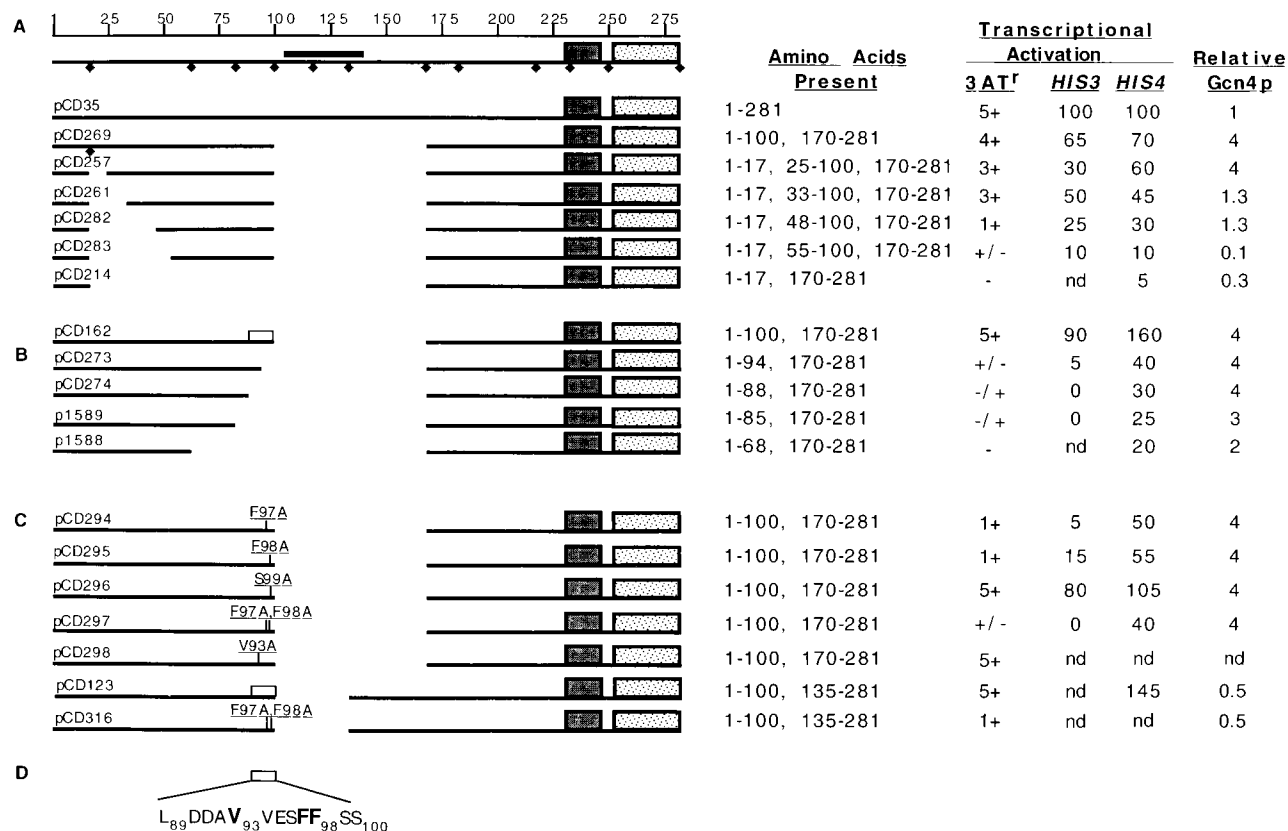


FIG. 6. Mutational analysis of the NTAD. The schematics and presentation of results are all as described in the legends to Fig. 2 and 5 except that the amino acid sequence shown in panel D and indicated by the open rectangles on constructs pCD162 and pCD123 contains the N-terminal portion of the motif proposed by Cress and Triezenberg (6). nd, not determined.

making a set of nested deletions in construct pCD162 (Fig. 6B). Deletions of only 6 to 12 residues from the C terminus of the NTAD in constructs pCD273 and pCD274 led to a marked reduction in transcriptional activation without decreasing the protein level relative to the pCD162 product (Fig. 6B and 4F). The deletion of 12 amino acids in pCD274 had a striking effect on *HIS3-lacZ* expression, reducing it to the level seen in the absence of GCN4, while leaving *HIS4-lacZ* expression at 30% of the wild-type level. The low-level activation of *HIS4* conferred by these two constructs was diminished further, but not completely eliminated, by removing an additional 20 residues from the C terminus of the NTAD (Fig. 6B, p1588). Together, the results in Fig. 6B indicate that an important component of the NTAD is located immediately upstream of the CAAD between residues 88 and 100; in the absence of this component, the remaining activation determinants located near the N terminus of the NTAD function poorly.

The 12 amino acids deleted in the pCD274 construct include the N-terminal one-third of the VP16 motif proposed for GCN4, including the hydrophobic residues Val-93, Phe-98, and three acidic residues (Fig. 6D). Given that critical phenylalanines occur in each of two separate acidic activation domains in VP16 (45), we made alanine substitutions of both Phe-97 and Phe-98, as well as of Val-93, in construct pCD162 (Fig. 6C). The results showed that a double substitution of Phe-97 and Phe-98 led to the same large reduction in transcriptional activation observed for deletion of residues 95 to 100 from pCD162 (Fig. 6B and C, compare pCD297 and pCD273). Each of the single-alanine substitutions of Phe-97 and Phe-98 re-

duced transcription significantly but had lesser effects than did the double mutation (pCD294 and pCD295 [Fig. 6C]). By contrast, substitution of Val-93 had little effect on transcriptional activation, as did the substitution of Ser-99 that we constructed as a negative control (pCD298 and pCD296 [Fig. 6C]). None of these point mutations had any effect on protein levels relative to that of the parental construct pCD162 (Fig. 6C and 4F). These results indicate that Phe-97 and Phe-98 each make important contributions to the activation function of the NTAD, whereas Val-93 does not.

Importance of hydrophobic amino acids in full-length GCN4. The results described above established that Phe-97 and Phe-98 are critical for activation by constructs lacking the entire CAAD and that Met-107, Tyr-110, Leu-113, Trp-120, Leu-123, and Phe-124 are important for the function of constructs lacking the entire NTAD. We wished to determine the effect of eliminating all eight of these bulky hydrophobic residues in an otherwise wild-type *GCN4* allele. As expected from the fact that the CAAD and the NTAD are independently sufficient for transcriptional activation, the double-alanine substitution of Phe-97 and Phe-98 (pCD324), the triple substitution of Met-107, Tyr-110, and Leu-113 (pCD321), and the triple substitution of Trp-120, Leu-123, and Phe-124 (pCD353) had little or no effect on GCN4 function relative to that of the parental construct pCD323 when these groups of mutations were present individually (Fig. 7A). Combining alanine substitutions of Phe-97, Phe-98, Met-107, Tyr-110, and Leu-113 in the same allele (pCD322) led to a small decrease in transcription relative to that of the parental construct pCD323, and

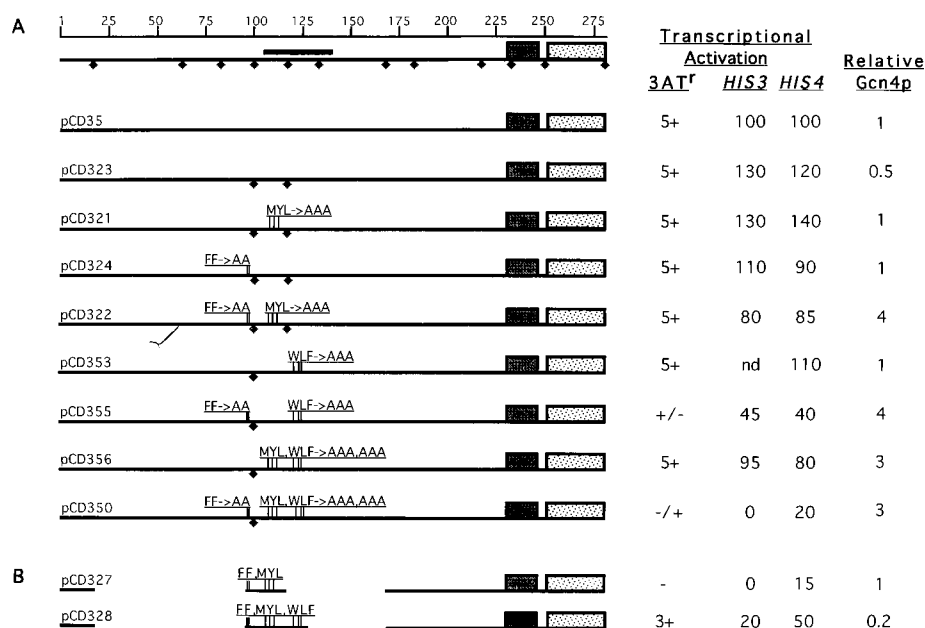


FIG. 7. Mutational analysis of bulky hydrophobic residues in the activation domain of full-length GCN4. The schematics and presentation of results are all as described in the legends to Fig. 2, 5, and 6. (A) Constructs pCD323, pCD321, pCD324, and pCD322 contain two *Bgl*II sites (solid diamonds shown below the sequences) inserted between residues 100 and 101 and 117 and 118. Constructs pCD353, pCD355, pCD356, and pCD350 contain a *Bgl*II site inserted between residues 117 and 118 (solid diamonds shown below the sequences). Constructs pCD321, pCD322, pCD356, and pCD350 have the same amino acid substitutions as pCD345 (Fig. 5B). Constructs pCD324, pCD322, pCD355, and pCD350 have the same amino acid substitutions as pCD297 (Fig. 6C). Constructs pCD353, pCD355, pCD356, and pCD350 have the same amino acid substitutions as pCD349 (Fig. 5B). (B) Constructs pCD327 and pCD328 contain wild-type *GCN4* residues 95 to 117 and 95 to 134, respectively, linked to residues 170 to 281. nd, not determined.

combining the substitutions at Trp-120, Leu-123, and Phe-124 with those at Phe-97 and Phe-98 produced a marked reduction in GCN4 function (pCD355 [Fig. 7A]). The fact that pCD355 shows a greater reduction in activation compared with pCD356 is in accord with the idea that defects in the CAAD and NTAD must be combined to observe a significant reduction in *GCN4* function. The fact that pCD355 is significantly more defective than pCD322 provides additional evidence that the activation subdomain containing Trp-120, Leu-123, and Phe-124 is more potent than that containing Met-107, Tyr-110, and Leu-113. When all eight substitutions were combined in the same allele, the resulting GCN4 protein was completely inactive at *HIS3* and gave only 20% of the wild-type activation at *HIS4* (pCD350 [Fig. 7A]). Together, these results show that the three clusters of hydrophobic residues we identified in the CAAD and NTAD make additive contributions to transcriptional activation by full-length GCN4.

Construct pCD350, which contains alanine substitutions of all eight hydrophobic residues and retains little activation function (Fig. 7A), had a dominant-negative phenotype when introduced into strain H1486 containing the wild-type *GCN4* chromosomal allele, diminishing 3-AT resistance relative to that seen following the introduction of vector DNA alone (data not shown). The same result was obtained for construct pCD346 (Fig. 5B) lacking the NTAD and the five hydrophobic residues in the CAAD and for pCD297 (Fig. 6C) lacking the CAAD and the Phe-97 and Phe-98 in the NTAD. These latter findings imply that the GCN4 proteins containing mutations in key hydrophobic residues in the activation domain are expressed efficiently, enter the nucleus, and interfere with the ability of native GCN4 to bind to its target genes or to activate transcription.

Finally, having shown that the eight hydrophobic residues in the interval 97 to 124 were necessary for the function of full-

length GCN4, we asked whether this segment was sufficient for activation. As shown in Fig. 3 and 7B, construct pCD328 containing residues 95 to 134 showed significant activation even though it was expressed at relatively low levels. In contrast, pCD327 containing residues 95 to 117 but lacking the critical amino acids Trp-120, Leu-123, and Phe-124 was completely inactive at *HIS3* and showed severely reduced activation of *HIS4* (Fig. 3). Taken together with other results, these findings indicate that the 97 to 124 interval contains at least two activation modules that can cooperate to promote efficient transcription in the absence of all other activation subdomains of GCN4.

Overexpression of GCN4 proteins containing the NTAD is toxic. Removing the four uORFs from the mRNA leader of the wild-type *GCN4* gene leads to constitutive high-level expression of *GCN4*, independent of amino acid availability (14). We found that overexpression of wild-type GCN4 protein in this fashion leads to a significant slow-growth phenotype on nutrient-rich medium (Fig. 8, p238). Interestingly, overexpression of the *GCN4* alleles shown in Fig. 2B, containing deletions in the CAAD but retaining the NTAD, led to even greater growth inhibition than occurred with overexpression of the wild-type coding sequences. In fact, the overexpressed derivative of construct pCD162 was lethal. The toxicity of the overexpressed derivative of pCD162, called pCD171, was eliminated completely by a two-codon insertion in the bZIP region (Fig. 8, pCD288). Importantly, construct pCD288 produced high constitutive levels of GCN4 protein (data not shown). The same results were obtained when a *Bgl*II insertion was made in the bZIP region of the construct that overexpresses wild-type GCN4 (Fig. 8, pCD118). These results indicate that the toxic effects of overproducing wild-type GCN4 or the mutant encoded by the pCD162 and pCD171 constructs require an intact DNA-binding domain in the overproduced proteins.

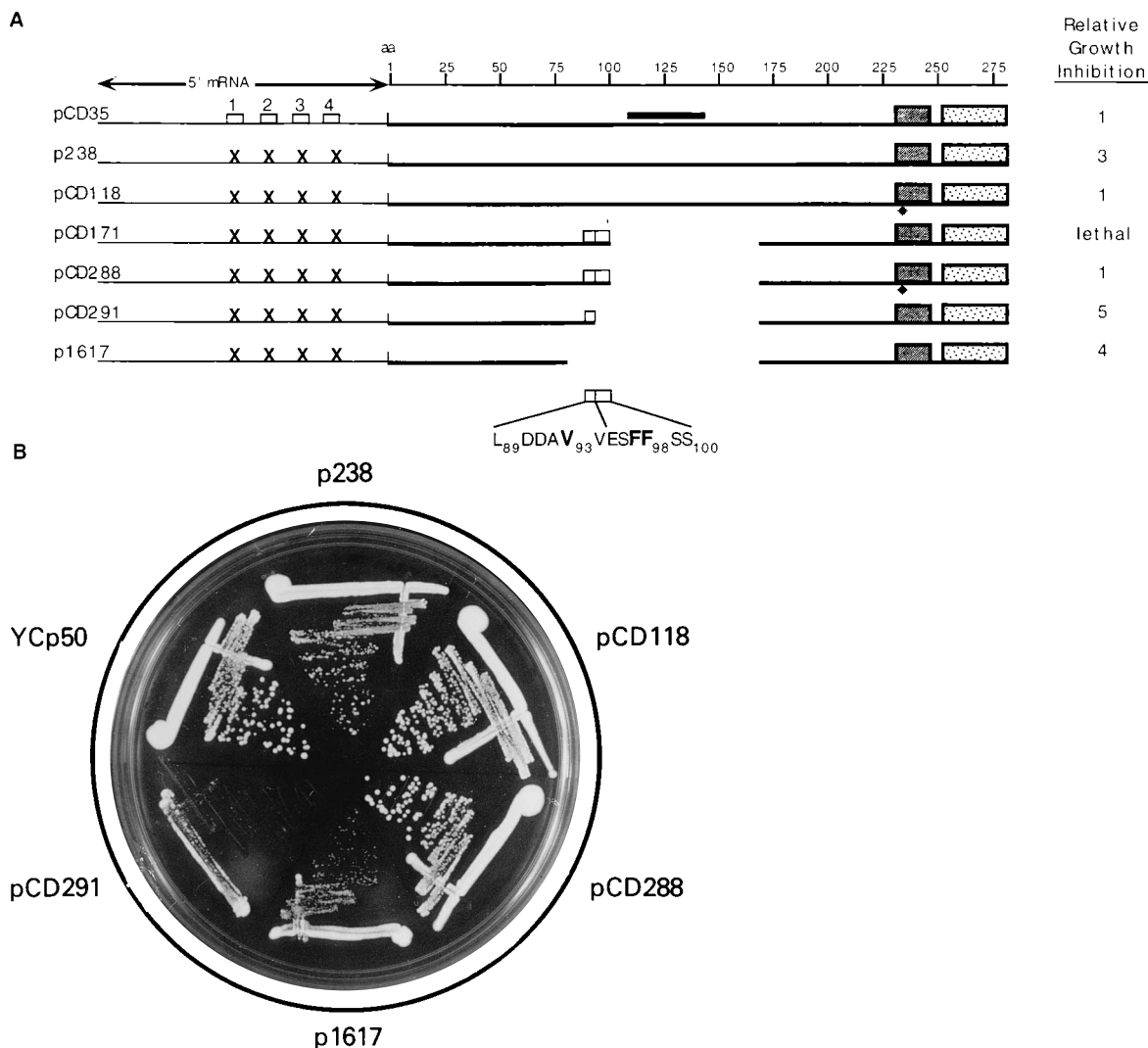


FIG. 8. Overexpression of wild-type and mutant GCN4 proteins is growth inhibitory under nonstarvation conditions. (A) Constructs p238, pCD171, p291, and p1617 were derived from pCD35 (wild type), pCD162, pCD273, and p1589, respectively (Fig. 6A and B), by deleting the four uORFs in the *GCN4* mRNA leader to permit overexpression of the encoded GCN4 proteins. Construct pCD118 was derived from p238 by insertion of a *Bgl*II site in the bZIP region at the same position as that present in construct pCD46 (Fig. 2A). Construct pCD288 was derived from pCD171, by making the same *Bgl*II insertion in the bZIP region. Relative growth inhibition was determined for single colonies on SC-Ura plates after introduction of the indicated constructs into the *gcn4* Δ strain H2032 (*MATa ura3-52 his1-29 leu2-3 leu2-112 trp1-63 gcn4::LEU2*). Growth inhibition was scored relative to that of wild-type GCN4 expressed at low levels (pCD35; no growth inhibition, score = 1). Scores higher than 1 indicate growth inhibition. (B) Transformants of H2032 bearing the constructs depicted in panel A or vector YCp50 alone were streaked on minimal medium supplemented with all 20 amino acids (aa; SC-Ura) and incubated for 2 days at 30°C. Transformants bearing the uORF-less version of pCD162 (pCD171) could not be analyzed, because this construct is lethal.

As shown in Fig. 6B, the deletions in constructs pCD273 and p1589 led to a progressive decrease in transcriptional activation while having little or no effect on the level of GCN4 protein relative to that of the parental construct pCD162. Overexpression of these two mutant proteins from constructs pCD291 and p1617 was not lethal, and the p1617 construct was less toxic than was pCD291 (Fig. 8). Thus, the effect of the pCD171 construct was progressively decreased by deletions in the C-terminal portion of the NTAD that diminished its activation function. The dependence of the lethal phenotype of pCD171 on both an intact DNA-binding domain and activation functions of the mutant protein suggests that overexpression of the NTAD sequesters one or more general transcription factors required for the expression of an essential gene (44). The fact that constructs pCD291 and p1617 are not lethal

but still exhibited a slow-growth phenotype (Fig. 8B) suggests that residues in the NTAD both C terminal and N terminal to the deletion junction in p1589 and p1617 (at residue 85) are capable of sequestering an important transcription factor.

Some of the constructs with deletions in the CAAD might be more toxic than construct p238 (which overexpresses wild-type GCN4) because the mutant proteins appear to be more stable than wild-type GCN4 (Fig. 2B, pCD109 and pCD162). However, other mutant proteins listed in Fig. 2B were more toxic than wild-type GCN4 when overexpressed (Δ uORF versions of pCD108, pCD123, and pCD110 [data not shown]) but were not present at levels in excess of wild-type GCN4 when expressed from constructs containing uORFs. These last findings raise the possibility that certain deletions in the CAAD can alter the

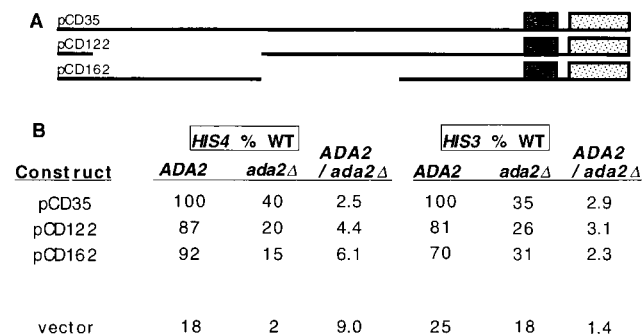


FIG. 9. The NTAD and CAAD have similar dependencies on ADA2 for transcriptional activation. *GCN4* deletion alleles were analyzed for the ability to activate transcription from *HIS3-lacZ* and *HIS4-lacZ* reporter genes in isogenic *ADA2* and *ada2* Δ strains (H2452, H2505, H2453, and H2506). Expression of each fusion is given as the percentage of that seen in the transformant bearing the wild-type (WT) construct pCD35 in the *ADA2* strain. The *GCN4*-independent expression seen in the strains transformed with vector alone is given on the bottom line and has not been subtracted from the other values. The *ADA2* dependence of transcriptional activation is indicated by the ratio of fusion gene expression in the *ADA2* strain to that observed in the *ada2* Δ strain (*ADA2/ada2* Δ).

structure of GCN4 in a way that increases the ability of the NTAD to bind and sequester general transcription factors.

The NTAD and CAAD are both dependent on ADA2 for efficient transcriptional activation. The *ADA2* gene was identified in a genetic selection for mutations that suppress the toxicity of overexpressing the VP16 activation domain fused to the GAL4 DNA-binding domain. It was proposed that GAL4-VP16 sequesters a general transcription factor in DNA-bound complexes in a way that requires the participation of ADA2. Subsequently, it was found that an *ada2* deletion decreases the efficiency of transcriptional activation by GCN4 as well as by GAL4-VP16 (2). On the basis of these findings, we asked whether the toxic effects of different overexpressed *GCN4* alleles could be overcome by *ada2* mutations. We found that none of the overexpressed versions of the *GCN4* constructs produced transformants that grew better, relative to the empty vector, in an *ada2-1* mutant versus the isogenic *ADA2* strain. The same result was obtained with a pair of isogenic *ada2* Δ (H2483) and *ADA2* (H2032) strains. Therefore, if the toxic effects of overexpressing *GCN4* arise from sequestration of a general transcription factor in nonproductive complexes, this phenomenon does not appear to require ADA2.

We asked next whether the NTAD and the CAAD were each dependent on ADA2 for transcriptional activation. In strains containing wild-type *GCN4* on construct pCD35, deletion of *ADA2* reduced *HIS4-lacZ* and *HIS3-lacZ* expression by factors of 2.5 and 2.9, respectively (Fig. 9), in agreement with previous findings for *HIS4* (2). Constructs pCD122 and pCD162, containing only the CAAD or the NTAD, respectively, gave results similar to those obtained with pCD35, except that pCD162 seemed to show somewhat greater dependence on ADA2 for transcription at *HIS4* than did pCD122 or pCD35. The levels of GCN4 proteins expressed from the constructs pCD35, pCD122, and pCD162 were indistinguishable between the *ada2* Δ and *ADA2* strains (data not shown). Therefore, the NTAD and the CAAD are each dependent on ADA2 for efficient transcriptional activation of *HIS3* and *HIS4*. It is remarkable that the basal-level transcription seen at *HIS4* in the absence of *GCN4* shows strong dependence on ADA2, whereas the *GCN4*-independent transcription at *HIS3* is essentially ADA2 independent (Fig. 9B, vector). The *GCN4*-

independent expression from *HIS4* has been attributed to the BAS1 and GRF10 (also known as BAS2 and PHO2) proteins (1); therefore, our results lead to the interesting conclusion that efficient transcriptional activation by these two proteins is ADA2 dependent. A specific activator required for basal transcription of *HIS3* has not been identified.

DISCUSSION

GCN4 contains two multipartite activation domains of similar potencies. The mutational analysis carried out by Struhl and colleagues (17, 18) localized a major activation function of GCN4 to ca. 40 amino acids in the center of the protein, at a location where the content of acidic amino acids is particularly high. Their results suggested that this domain consists of multiple activation subdomains, and they proposed that the net negative charge of the combined subdomains was a critical determinant of GCN4 activation function. We confirmed the existence of a potent activation domain in the center of GCN4 (the CAAD) and identified six bulky hydrophobic residues in this domain (Met-107, Tyr-110, Leu-113, Trp-120, Leu-123, and Phe-124) that are critical for function when the CAAD is the sole activation domain in GCN4. Hope et al. (17) found that deletion of residues C terminal to the six critical hydrophobic residues we identified in the CAAD almost completely destroyed activation in constructs lacking the NTAD. This suggests that the C-terminal half of the CAAD (positions 124 to 147) is also important for activation by this domain. It will be interesting to determine whether this C-terminal segment of the CAAD is dependent on hydrophobic amino acids or whether the high levels of acidic residues in this subdomain account for its contribution to activation. The importance of individual acidic amino acids located in other parts of the CAAD and throughout the NTAD should also be addressed.

While it was noted previously that GCN4 contains additional activation determinants in the N-terminal region that can partially compensate for removal of a substantial portion of the CAAD (17, 42), the NTAD had not been investigated systematically until now. We found that this domain can confer high-level transcription in the complete absence of the CAAD when *GCN4* is expressed under its native promoter and translational control elements. Our results indicate that the NTAD occupies most of the N-terminal 100 amino acids of GCN4. Its N-terminal boundary was placed in the vicinity of residues 17 to 25, on the basis of the deletions in constructs pCD269 and pCD257 (Fig. 6A). The C-terminal boundary of the NTAD was established more precisely by the fact that deleting only six amino acids from the C terminus of the NTAD in construct pCD273 led to a substantial decline in activation relative to that in pCD162 (Fig. 6B). The important activation function present at the extreme C terminus of the NTAD is dependent on residues Phe-97 and Phe-98.

Although a complete deletion of the CAAD in construct pCD162 left high-level transcription intact, this construct produced levels of GCN4 protein higher than wild-type levels (Fig. 2B and 6B). However, constructs pCD213 and pCD196 that contain only the NTAD or the CAAD, respectively, linked directly to the bZIP domain conferred nearly equivalent levels of transcriptional activation, even though construct pCD213 was expressed at lower levels than pCD196 (Fig. 2F and 3). These latter results indicate that the NTAD and CAAD function comparably at low levels of GCN4 protein when all the binding sites at its target genes are unlikely to be filled. When the proteins encoded by pCD213 and pCD196 were overexpressed by removal of the uORFs from these two constructs, transcription of the *HIS3-lacZ* and *HIS4-lacZ* fusions in-

creased by comparable amounts for the two *GCN4* alleles and exceeded by a factor of 2 to 3 the level of expression conferred by the wild-type *GCN4* (data not shown). Another indication that the NTAD is a potent activation domain is that overexpression of this region has a toxic effect on cell growth. This toxicity appears to result from sequestration of one or more general transcription factors because it was completely dependent on an intact DNA-binding domain and was diminished in degree when activation by the NTAD was compromised by small deletions from the C terminus. It is noteworthy that significant toxicity was evident for constructs pCD291 and p1617 that lack the C-terminal portion of the NTAD, including the important residues Phe-97 and Phe-98 (Fig. 8). This latter finding suggests that the remaining N-terminal residues in the NTAD are capable of sequestering a general transcription factor independently of the potent activation determinants located between residues 85 and 100.

It is interesting that pCD162, and most of our other constructs containing a deletion in the interval between residues 135 and 185, produced levels of GCN4 protein higher than wild-type levels (pCD109, pCD162, pCD112, and pCD116 [Fig. 2] and pCD270 and pCD271 [Fig. 5A]). These findings raise the possibility that residues located within the CAAD and between the CAAD and bZIP regions promote proteolytic degradation of the protein. This function may be important in returning the GCN4 protein to low levels when amino acids are replenished following its induction in response to an amino acid limitation (53). It is also noteworthy that multiple electrophoretic species of GCN4 protein were detected by immunoblot analysis (Fig. 4). We do not know whether these different isoforms were produced by proteolysis or by some form of covalent modification.

Clusters of hydrophobic residues in the NTAD and CAAD are critical for transcriptional activation. Mutational analyses of the activation domains of VP16 (6, 45), Epstein-Barr virus Rta protein (13), p53 (32), Sp1 (10), c-Fos (36), E1a (31), and GAL4 (30) have shown that bulky hydrophobic residues in these proteins are essential for transcriptional activation. Cress and Triezenberg (6) suggested that the critical hydrophobic residues and surrounding acidic amino acids in VP16 compose a sequence motif that is loosely conserved between VP16 and other transcriptional activators, including GCN4. Prior to this analysis, the importance of this proposed motif in GCN4 had not been addressed. We found that Phe-97 and Phe-98, located in the N terminus of the VP16-related motif, are important for transcriptional activation by the NTAD (Fig. 6C) and that the other bulky hydrophobic residues in the proposed motif (Met-107, Tyr-110, and Leu-113) make strong contributions to the function of the CAAD (Fig. 5B and C). These findings suggest that the GCN4 activation domain has important structural features in common with VP16 and other transcriptional activators. We obtained evidence that certain acidic residues in the CAAD are also required for efficient activation. There are several indications that the cluster of hydrophobic residues Trp-120, Leu-123, and Phe-124 is even more important for transcriptional activation than are the residues between Phe-97 and Leu-113 highlighted by Cress and Triezenberg (Fig. 5B). The fact that Trp-120, Leu-123, and Phe-124 are conserved between GCN4 and *Neurospora cpc-1* also suggests that they have a prominent role in the activation function of the CAAD. We cannot determine from our data whether the alanine substitutions of hydrophobic residues alter the overall structure of the activation domain or impair specific contacts between GCN4 and coactivators or basic transcription factors. It is worth noting, however, that certain transcription factors contain critical hydrophobic residues, including TBP (22) and

TAF_{II}230 (25), and it has been suggested that hydrophobic interactions are important in stabilizing contacts between transcriptional activators and their targets in the transcriptional machinery (6, 52).

The VP16-related motif spanning residues 95 to 117 in GCN4 is divided between the C terminus of the NTAD and the N terminus of the CAAD. Because these domains are only defined operationally as contiguous segments that can promote wild-type transcriptional activation, it is possible that the important residues in the C terminus of the NTAD and the N terminus of the CAAD cooperate in wild-type GCN4 to carry out a single step in the activation process. If so, they can also cooperate with other activation subdomains located more N terminal in the NTAD or C terminal in the CAAD, because they are required for the function of constructs like pCD162 and pCD122 that contain only the NTAD or the CAAD. In fact, the results from constructs pCD327 and pCD328 in Fig. 7B and 3 show that segment 95 to 117 containing the VP16-related motif is nonfunctional when present alone in GCN4, requiring the segment containing Trp-120, Leu-123, and Phe-124 to achieve significant activation.

The fact that a construct containing point mutations in all five critical hydrophobic residues in the 95 to 117 interval of full-length GCN4 (pCD322 [Fig. 7A]) retains high-level activation indicates that the entire VP16-related domain is dispensable in the presence of other segments of the activation domain. Activation in the absence of the VP16-related motif is critically dependent on Trp-120, Leu-123, and Phe-124, because full-length GCN4 protein lacking all eight hydrophobic residues in the 95 to 124 interval (pCD350) is almost completely inactive (Fig. 7A). The fact that construct pCD125 (Fig. 5A and 3), which lacks the NTAD in addition to the VP16-related subdomain, is substantially more impaired than is pCD322 (Fig. 7A) implies that sequences in the NTAD located N terminal to Phe-97 and Phe-98 can cooperate with the segment of the CAAD containing Trp-120, Leu-123, and Phe-124 to achieve efficient transcriptional activation. The results in Fig. 5B and 7B demonstrate that the subdomain containing Trp-120, Leu-123, and Phe-124 can similarly cooperate with some or all of the elements of the VP16-related motif. Thus, we conclude that the NTAD and CAAD each contain multiple subdomains that can cooperate in different combinations to promote efficient transcriptional activation of GCN4-dependent promoters.

The importance of functional redundancy in transcriptional activation by GCN4. What is the significance of the extensive functional redundancy evident in the GCN4 activation domain? One possibility is that different segments of the activation domain interact with different proteins in the transcriptional machinery. For example, there is evidence that VP16 interacts with TBP (20, 51), TFIIB (33, 34, 46), and TAF_{II}40 (11). If GCN4 can interact with several different proteins in the initiation complex, or with certain chromatin proteins, this would help to explain why large segments of its activation domain can be deleted without greatly reducing the expression of at least some of its target genes. Because GCN4 must activate transcription from a large number of genes (upwards of 50 [14]), it may also need to interact with different transcription factors at different promoters. Presumably, the *HIS4* promoter will be bound by BAS1 and GRF10, two proteins required for basal transcription of this gene, when GCN4 binds under amino acid starvation conditions. BAS1 and GRF10 may supply certain stimulatory interactions with the transcriptional machinery that GCN4 does not have to provide in order to achieve high-level activation of the *HIS4* promoter. In general, we found that expression of the *HIS3-lacZ* fusion was impaired

to a greater extent than was *HIS4-lacZ* for GCN4 constructs containing only a portion of the NTAD or CAAD (e.g., pCD313 in Fig. 5C and pCD297 in Fig. 6C). Perhaps the *HIS3* gene, which does not utilize BAS1 and GRF10 for its basal expression, has a greater requirement for multiple activation determinants in GCN4, or for a particular segment of the GCN4 activation domain, to attain high-level activation. Interestingly, we have indications that under starvation conditions more severe than those used in this study, neither the NTAD nor the CAAD alone is sufficient for a wild-type level of activation of some genes in the *HIS* pathway (data not shown).

An alternative way to explain the stronger effects of mutations in the GCN4 activation domain on expression of *HIS3* versus *HIS4* would be to propose that *HIS3* has fewer GCN4 binding sites. An assumption of this model is that a particular activation subdomain is flexible enough to interact with more than one target in the transcriptional machinery, as appears to be the case for one of the VP16 activation domains (11, 20, 33, 34, 51). At *HIS4*, binding of several mutant proteins containing only one or two functional activation subdomains would permit multiple stimulatory interactions to occur, thereby achieving a high level of activation. At *HIS3*, by contrast, binding of only a single molecule of a mutant protein lacking certain subdomains would not provide a sufficient number of interactions for high-level transcription. In fact, there is evidence that more high-affinity GCN4 binding sites are present at *HIS4* than at *HIS3* (14). The point mutations described here that impair particular activation subdomains in GCN4 should eventually allow us to identify which components of the transcriptional machinery are contacted by each of the subdomains and thereby bring us closer to an understanding of how GCN4 activates transcription.

ACKNOWLEDGMENTS

We thank K. Natarajan, Neal Silverman, and Carl Wu for helpful comments on the manuscript.

REFERENCES

- Arndt, K. T., C. Styles, and G. R. Fink. 1987. Multiple global regulators control *HIS4* transcription in yeast. *Science* **237**:874–880.
- Berger, S. L., B. Piña, N. Silverman, G. A. Marcus, J. Agapite, J. L. Regier, S. J. Triezenberg, and L. Guarente. 1992. Genetic isolation of ADA2: a potential transcription adaptor required for function of certain acidic domains. *Cell* **70**:251–265.
- Boeke, J. D., J. Trueheart, G. Natsoulis, and G. R. Fink. 1987. 5-Fluoroorotic acid as a selective agent in yeast molecular genes. *Methods Enzymol.* **154**: 164–175.
- Bradford, M. M. 1976. A rapid and sensitive method for the quantitation of microgram quantities of protein utilizing the principle of protein-dye binding. *Anal. Biochem.* **72**:248–254.
- Buratowski, S. 1994. The basics of basal transcription by RNA polymerase II. *Cell* **77**:1–3.
- Cress, W. D., and S. J. Triezenberg. 1991. Critical structural elements of the VP16 transcriptional activation domain. *Science* **251**:87–90.
- Ellenberger, T. E., C. J. Brandl, K. Struhl, and S. C. Harrison. 1992. The GCN4 basic region leucine zipper binds DNA as a dimer of uninterrupted α helices: crystal structure of the protein-DNA complex. *Cell* **71**:1223–1237.
- Geisberg, J. V., W. S. Lee, A. J. Berk, and R. P. Ricciardi. 1994. The zinc finger region of the adenovirus E1A transactivating domain complexes with the TATA box binding protein. *Proc. Natl. Acad. Sci. USA* **91**:2488–2492.
- Georgakopoulos, T., and G. Thireos. 1992. Two distinct yeast transcriptional activators require the function of the GCN5 protein to promote normal levels of transcription. *EMBO J.* **11**:4145–4152.
- Gill, G., E. Pascal, Z. H. Tseng, and R. Tjian. 1994. A glutamine-rich hydrophobic patch in transcription factor Sp1 contacts the dTAF_{II}110 component of the *Drosophila* TFIID complex and mediates transcriptional activation. *Proc. Natl. Acad. Sci. USA* **91**:192–196.
- Goodrich, J. A., T. Hoey, C. J. Thut, A. Admon, and R. Tjian. 1993. *Drosophila* TAF_{II}40 interacts with both a VP16 activation domain and the basal transcription factor TFIIB. *Cell* **75**:519–530.
- Hahn, S. 1993. Structure (?) and function of acidic transcription activators. *Cell* **72**:481–483.
- Hardwick, J. M., L. Tse, N. Applegren, J. Nicholas, and M. A. Veluona. 1992. The Epstein-Barr virus R transactivator (Rta) contains a complex, potent activation domain with properties different from those of VP16. *J. Virol.* **66**:5500–5508.
- Hinnebusch, A. G. 1992. General and pathway-specific regulatory mechanisms controlling the synthesis of amino acid biosynthetic enzymes in *Saccharomyces cerevisiae*, p. 319–414. In E. W. Jones, J. R. Pringle, and J. R. Broach (ed.), *The molecular and cellular biology of the yeast Saccharomyces*: gene expression. Cold Spring Harbor Laboratory Press, Cold Spring Harbor, N.Y.
- Hinnebusch, A. G., and G. R. Fink. 1983. Positive regulation in the general amino acid control of *Saccharomyces cerevisiae*. *Proc. Natl. Acad. Sci. USA* **80**:5374–5378.
- Hoey, T., R. O. J. Weinzierl, G. Gill, J. Chen, R. D. Dynlacht, and R. Tjian. 1993. Molecular cloning and functional analysis of *Drosophila* TAF_{II}110 reveal properties expected of coactivators. *Cell* **72**:247–260.
- Hope, I. A., S. Mahadevan, and K. Struhl. 1988. Structural and functional characterization of the short acidic transcriptional activation region of yeast GCN4 protein. *Nature (London)* **333**:635–640.
- Hope, I. A., and K. Struhl. 1986. Functional dissection of a eukaryotic transcriptional activator protein, GCN4 of yeast. *Cell* **46**:885–894.
- Hope, I. A., and K. Struhl. 1987. GCN4, a eukaryotic transcriptional activator protein, binds as a dimer to target DNA. *EMBO J.* **6**:2781–2784.
- Ingles, C. J., M. Shales, W. D. Cress, S. J. Triezenberg, and J. Greenblatt. 1991. Reducing binding of TFIID to transcriptionally compromised mutants of VP16. *Nature (London)* **351**:588–590.
- Innes, M. A., D. H. Gelfand, J. J. Sninsky, and T. J. White. 1990. PCR protocols. Academic Press, Inc., San Diego, Calif.
- Kim, T. K., S. Hashimoto, R. J. Kelleher, P. M. Flanagan, R. D. Kornberg, M. Horikoshi, and R. G. Roeder. 1994. Effects of activation-defective TBP mutations on transcription initiation in yeast. *Nature (London)* **369**:252–255.
- Kim, Y., S. Bjorklund, Y. Li, M. H. Sayre, and R. D. Kornberg. 1994. A multiprotein mediator of transcriptional activation and its interaction with the C-terminal repeat domain of RNA polymerase II. *Cell* **77**:599–608.
- Kinney, D. M., and C. J. Lusty. 1989. Arginine restriction induced by *d*-N-(phosphonacetyl)-L-ornithine increased expression of *HIS3*, *TRP5*, *CPA1*, and *CPA2* in *Saccharomyces cerevisiae*. *Mol. Cell. Biol.* **9**:4882–4888.
- Kokubo, T., S. Yamashita, M. Horikoshi, R. Roeder, and Y. Nakatani. 1994. Interaction between the N-terminal domain of the 230-kDa subunit and the TATA box-binding subunit of TFIID negatively regulates TATA-box binding. *Proc. Natl. Acad. Sci. USA* **91**:3520–3524.
- Koleske, A. J., and R. A. Young. 1994. An RNA polymerase II holoenzyme responsive to activators. *Nature (London)* **368**:466–469.
- Laemmli, U. 1970. Cleavage of structural proteins during the assembly of the head of bacteriophage T4. *Nature (London)* **227**:680–685.
- Landschulz, W. H., P. F. Johnson, and S. L. McKnight. 1988. The leucine zipper: a hypothetical structure common to a new class of DNA binding proteins. *Science* **240**:1759–1764.
- Leuther, K. K., and S. A. Johnston. 1992. Nondissociation of GAL4 and GAL80 in vivo after galactose induction. *Science* **256**:1333–1335.
- Leuther, K. K., J. M. Salmeron, and S. A. Johnston. 1993. Genetic evidence that an activation domain of GAL4 does not require acidity and may form a β sheet. *Cell* **72**:575–585.
- Lillie, J. W., and M. R. Green. 1989. Transcription activation by the adenovirus E1a protein. *Nature (London)* **338**:39–44.
- Lin, J., J. Chen, B. Elenbaas, and A. J. Levine. 1994. Several hydrophobic amino acids in the p53 amino-terminal domain are required for transcriptional activation, binding to mdm-2 and the adenovirus 5 E1B 55-kD protein. *Genes Dev.* **8**:1235–1246.
- Lin, Y., and M. R. Green. 1991. Mechanism of action of an acidic transcriptional activator in vitro. *Cell* **64**:971–981.
- Lin, Y., I. Ha, E. Maldonado, D. Reinberg, and M. R. Green. 1991. Binding of general transcription factor TFIIB to an acidic activating region. *Nature (London)* **353**:569–571.
- Ma, J., and M. Ptashne. 1987. Deletion analysis of *GAL4* defines two transcriptional activating segments. *Cell* **48**:847–853.
- Metz, R., A. J. Bannister, J. A. Sutherland, C. Hagemeyer, E. C. O'Rourke, A. Cook, R. Bravo, and T. Kouzarides. 1994. C-Fos-induced activation of a TATA-box-containing promoter involves direct contact with TATA-binding protein. *Mol. Cell. Biol.* **14**:6021–6029.
- Miller, P., C. Grant, and A. Hinnebusch. Unpublished data.
- Moehle, C. M., and A. G. Hinnebusch. 1991. Association of RAP1 binding sites with stringent control of ribosomal protein gene transcription in *Saccharomyces cerevisiae*. *Mol. Cell. Biol.* **11**:2723–2735.
- Mueller, P. P., and A. G. Hinnebusch. 1986. Multiple upstream AUG codons mediate translational control of *GCN4*. *Cell* **45**:201–207.
- Nasmyth, K., and K. Tatchell. 1980. The structure of transposable yeast mating type loci. *Cell* **19**:753–764.
- O'Shea, E. K., J. D. Klemm, P. S. Kim, and T. Alber. 1991. X-ray structure of the GCN4 leucine zipper, a two-stranded, parallel coiled coil. *Science* **254**:539–544.
- Paluh, J. L., M. J. Orbach, T. L. Legerton, and C. Yanofsky. 1988. The

- cross-pathway control gene of *Neurospora crassa*, *cpc-1*, encodes a protein similar to GCN4 of yeast and the DNA-binding domain of the oncogene *v-jun*-encoded protein. Proc. Natl. Acad. Sci. USA **85**:3728–3732.
42. **Pellman, D., M. E. McLaughlin, and G. R. Fink.** 1990. TATA-dependent and TATA-independent transcription at the *HIS4* gene of yeast. Nature (London) **348**:82–85.
 43. **Promega Corporation.** 1991. Promega protocols and applications guide, 2nd ed. Promega Corporation, Madison, Wis.
 44. **Ptashne, M., and A. A. F. Gann.** 1990. Activators and targets. Nature (London) **346**:329–331.
 45. **Regier, J. L., F. Shen, and S. J. Triezenberg.** 1993. Pattern of aromatic and hydrophobic amino acids critical for one of two subdomains of the VP16 transcriptional activator. Proc. Natl. Acad. Sci. USA **90**:883–887.
 46. **Roberts, S. G. E., I. Ha, E. Maldonado, D. Reinberg, and M. R. Green.** 1993. Interaction between an acidic activator and transcription factor TFIIB is required for transcriptional activation. Nature (London) **363**:741–744.
 47. **Seto, E., A. Usheva, G. P. Zambetti, J. Momand, N. Horikoshi, R. Weinmann, A. J. Levine, and T. Shen.** 1992. Wild-type p53 binds to the TATA-binding protein and represses transcription. Proc. Natl. Acad. Sci. USA **89**:12028–12032.
 48. **Shapira, S. K., J. Chou, F. V. Richaud, and M. J. Casadaban.** 1983. New versatile plasmid vectors for expression of hybrid proteins coded by a cloned gene fused to *lacZ* gene sequences encoding an enzymatically active carboxy-terminal portion of β -galactosidase. Gene **25**:71–82.
 49. **Sherman, F., G. R. Fink, and C. W. Lawrence.** 1974. Methods of yeast genetics. Cold Spring Harbor Laboratory, Cold Spring Harbor, N.Y.
 50. **Sikorski, R. S., and P. Hieter.** 1989. A system of shuttle vectors and yeast host strains designated for efficient manipulation of DNA in *Saccharomyces cerevisiae*. Genetics **122**:19–27.
 51. **Stringer, K. F., C. J. Ingles, and J. Greenblatt.** 1990. Direct and selective binding of an acidic transcription factor domain to the TATA-box factor TFIID. Nature (London) **345**:783–786.
 52. **Tjian, R., and T. Maniatis.** 1994. Transcriptional activation: a complex puzzle with few easy pieces. Cell **77**:5–8.
 53. **Tzamarias, D., I. Roussou, and G. Thireos.** 1989. Coupling of GCN4 mRNA translational activation with decreased rates of polypeptide chain initiation. Cell **57**:947–954.
 54. **Van Hoy, M., K. K. Leuther, T. Kodadek, and S. A. Johnston.** 1993. The acidic activation domains of the GCN4 and GAL4 proteins are not α helical but form β sheets. Cell **72**:587–594.
 55. **Vazquez de Aldana, C. R., R. C. Wek, P. San Segundo, A. G. Truesdell, and A. G. Hinnebusch.** 1994. Multicopy tRNA genes functionally suppress mutations in yeast eIF-2 α kinase GCN2: evidence for separate pathways coupling *GCN4* expression to uncharged tRNA. Mol. Cell. Biol. **14**:7920–7932.
 56. **Wek, R. C., J. F. Cannon, T. E. Dever, and A. G. Hinnebusch.** 1992. Truncated protein phosphatase *GLC7* restores translational activation of *GCN4* expression in yeast mutants defective for the eIF-2 α kinase GCN2. Mol. Cell. Biol. **12**:5700–5710.
 57. **Williams, N. P., P. P. Mueller, and A. G. Hinnebusch.** 1988. The positive regulatory function of the 5'-proximal open reading frames in *GCN4* mRNA can be mimicked by heterologous, short coding sequences. Mol. Cell. Biol. **8**:3827–3836.